[American Journal of Science, Vol. 304, January, 2004, P. 21–66]

THERMODYNAMIC PROPERTIES OF ANALCIME SOLID SOLUTIONS

PHILIP S. NEUHOFF*†,**, GUY L. HOVIS***, GIUSEPPINA BALASSONE****, and JONATHAN F. STEBBINS**

ABSTRACT. **Analcime ($Na_xAl_xSi_{3-x}O_6 \cdot [(3-x)/2]H_2O$, where x varies from ~0.78 to ~1.06) is one of the most common rock-forming zeolites. It forms in a wide range of geologic environments that span a range of temperature and pressure from ambient to magmatic conditions. Cluster variation method analysis of ^{29}Si magic angle spinning nuclear magnetic resonance spectra indicates 1) the presence of at least two distinct states of short range Si/Al disorder [low (less disordered) and high (more disordered) analcime], and 2) that configurational entropy associated short-range Si-Al disorder within each of these states increases regularly with increasing Si content. Hydrofluoric acid (HF) solution calorimetry at 50°C was used to determine the enthalpy of formation of five pure analcime samples of varying composition (range of x approximately 0.95 to 1.05) and Si-Al disorder. Enthalpies of formation from the elements at 25°C (ΔH_f) for these samples fall on a linear trend, except for one sample of high analcime for which ΔH_f was about 6.1 ± 3.0 kJ/mol less stable than a low analcime of the same composition. Comparison with the results of previous calorimetric studies indicates negligible excess enthalpies of mixing in both low and high analcime solid solutions (that is, the solid solutions are athermal). The configurational entropies derived from cluster variation analysis were in turn used to derive activity-composition relationships for low analcime solid solutions whose compositions are bounded by an aluminous endmember ($Na_{1.05}Al_{1.05}Si_{1.95}O_6 \cdot 0.975H_2O$) and a siliceous endmember ($Na_{0.75}Al_{0.75}Si_{2.25}O_6 \cdot 1.125H_2O$). These relationships were used to retrieve thermodynamic properties for the endmembers from experimental observations of equilibria between analcime, albite, and aqueous solutions. Retrieved values of ΔH_f are in excellent agreement with the calorimetric results of this study. Comparative analysis of equilibrium observations in the literature indicate that one sample of analcime from the Mont St. Hilaire alkaline intrusive complex used for analcime solubility measurements is high analcime. The Gibbs energy of disordering at 298.15 K, 1 bar consistent with the retrieval calculations is ~ 6 kJ/mol. The thermodynamic properties of disordering for analcime indicate that hydrated low analcime is stable with respect to hydrated high analcime everywhere in Earth's crust. Phase relations between low analcime, quartz, albite, and aqueous solutions calculated from the retrieved thermodynamic data indicate that at quartz equilibrium, low analcime should become more Si-rich with increasing temperature and pressure and that the composition of analcime is a sensitive function of the chemical potential of SiO_2. Stable equilibrium between analcime, albite, quartz and H_2O occurs at much lower temperatures than suggested by earlier phase equilibrium experiments. The breakdown of analcime plus quartz to form albite in geologic systems probably reflects metastable equilibrium in which the composition of analcime did not equilibrate with quartz.**

INTRODUCTION

Analcime ($Na_xAl_xSi_{3-x}O_6 \cdot [(3-x)/2]H_2O$, where x varies from ~0.78 to ~1.20) is one of the most common rock-forming zeolite minerals. The widespread occurrence of analcime is related to the fact that it appears to be stable over a considerable range of temperature and pressure conditions. Analcime is formed not only during burial

*Department of Geological Sciences, University of Florida, Gainesville, Florida 32611-2120
**Department of Geological and Environmental Sciences, Stanford University, Stanford, California 94305-2115
***Department of Geology and Environmental Geosciences, Lafayette College, Easton, Pennsylvania 18042
****Dipartimento di Scienze della Terra, Universita di Napoli, Naples, Italy
†Present address of corresponding author

diagenesis of volcanoclastic sediments and very-low grade metamorphism of lavas, as is observed with many zeolites, but also forms in saline, alkaline lakes at the surface of the earth as well as in pegmatitic and hydrothermal veins around alkaline intrusive complexes and as a phenocryst phase in silica-deficient igneous rocks (for example, Walker, 1960; Hay, 1966; Coombs and Whetten, 1967; Iijima, 1978, 1988; Broxton and others, 1987; Wilkinson and Hensel, 1994; Neuhoff and others, 1997; Markl and others, 2001). In all of these settings, the formation of analcime is very sensitive to chemical potential of SiO_2 (Saha, 1961; Coombs and Whetten, 1967; Wise, 1984) and potentially other thermodynamic components necessary for its formation (for example, H_2O, Na_2O, Al_2O_3, et cetera.). Understanding of phase relations involving analcime is thus critical for interpretation and modeling of mineral paragenesis in a number of geologic environments.

Numerous studies have determined equilibria between analcime and coexisting minerals and aqueous solutions (Campbell and Fyfe, 1965; Apps, ms, 1970; Thompson, 1971; Liou, 1971; Murphy and others, 1996, Wilkin and Barnes, 1998; Redkin and Hemley, 2000). However, interpretation and computation of equilibria involving analcime from these results are complicated by the presence of substantial solid solution. Relative to other zeolite minerals, however, the dominant solid solution observed in analcime is relatively simple. Outside of some relatively rare occurrences of Ca and Cs substitution for Na (see review in Passaglia and Sheppard, 2001), virtually all analcimes contain only Na^+ in the extraframework cation sites. Substitution of elements other than Al and Si is generally not observed. If one considers only the anhydrous framework, solid solution in analcime thus involves a direct substitution of $NaAlO_2$ for SiO_2 (see formula above). Controversy exists as to whether the H_2O content of analcime varies along this solid solution (Saha, 1959; Wise, 1984), but it is well established that analcime can be reversibly dehydrated at elevated temperatures and pressures (van Reeuwijk, 1974). The thermodynamic consequences of these solid solutions have received relatively little attention. Wise (1984) combined chemographic analysis of experimental and geologic phase relations with published calorimetric measurements and inferred a nearly linear dependence of the Gibbs energy of formation (ΔG_f) on the composition of analcime. Wise (1984) took this to indicate that analcime solid solutions were nearly ideal, although ΔG_f is not a linear function of composition in ideal solid solutions due to the non-linear nature of the entropy of mixing. More recently, Neuhoff and others (2003) proposed that analcime solid solutions obey an athermal solid solution model. In their model, the excess enthalpy of mixing (H^{EX}) is negligible and the excess entropy of mixing (S^{EX}) is finite, being constrained by the fitting of ^{29}Si magic angle spinning nuclear magnetic resonance (MAS NMR) results. Although the assumption that H^{EX} is negligible is consistent with the behavior of other highly symmetrical zeolites (Petrovic and Navrotsky, 1997; Shim and others, 1999), the calorimetric data necessary to test this hypothesis were not available.

The present study addresses this issue through determination of the enthalpy of formation of several analcime samples with differing composition by HF solution calorimetry. These results are used to confirm that H^{EX} is negligible for analcime solid solutions over a composition range exhibited by most natural samples. Activity-composition relations for analcime based on the athermal solution models of Neuhoff and Stebbins (2001) and Neuhoff and others (2003) and the calorimetric observations obtained in this study are then used as the basis for retrieval of the thermodynamic properties of analcime solid solutions. The resulting thermodynamic data and models are in excellent agreement with experimental equilibrium observations and the geologic occurrence of analcime.

SAMPLES AND CHARACTERIZATION

Samples

The samples used in the present study are listed in table 1. Sample identification and purity were confirmed through X-ray powder diffraction (XRPD) using a Rigaku theta-theta diffractometer with CuKα radiation operating at 35 kV and 15 mA. The analcime from the Mont St. Hilaire alkaline intrusive complex in Quebec was purchased from Ward's Natural Science as several 0.5 to 8 milligram grains of glassy to opaque analcime and hand picked to eliminate small inclusions of aegirine and other minerals. Two separates were produced from this sample: a glassy, optically transparent sample (ANA-MSHG) that was the same sample as ANA001 in Neuhoff and others (2003) and an opaque separate (ANA-MSHO). The two separates originally consisted of separate grains and it was unclear if there is any paragenetic relationship between

TABLE 1

Compositions and unit cell parameters of analcime samples in this study

Sample	ANA-MSHG	ANA-MSHO	ANA-SBC	ANA-BZI	ANA-MVI
Locality	Mont St. Hilaire, Canada	Mont St. Hilaire, Canada	San Benito Co., California	Bolzano, Italy	Mt. Vesuvius, Italy
			Oxide Weight Percents from EPMA[1]		
SiO_2	55.17	55.17	54.12	55.20	57.01
Al_2O_3	23.00	23.01	22.39	22.52	21.32
CaO	0.00	0.00	0.01	0.00	0.00
Na_2O	13.98	14.13	13.62	13.69	12.96
K_2O	0.00	0.00	0.33	0.00	0.00
total	92.16	92.31	90.47	91.41	91.28
			Anhydrous formula unit compositions from EPMA		
Si	2.01	2.01	2.01	2.03	2.08
Al	0.99	0.99	0.98	0.97	0.92
Ca	0	0.00	0	0	0
Na	0.99	1.00	0.98	0.97	0.92
K	0	0.00	0.02	0	0
O	6	6	6	6	6
			Si/Al Ratios		
$Si/Al_{(EPMA)}$[2]	2.04	2.04	2.05	2.08	2.27
$Si/Al_{(EPMA)}$ range[3]	1.94 – 2.06	1.95 – 2.02	1.91 – 2.06	1.97 – 2.06	2.19 – 2.26
$Si/Al_{(NMR)}$	1.95	–	1.86	1.91	2.17
			Water contents from thermogravimetry		
H_2O (wt%)	8.09 ± .03	8.10 ± .03	7.97 ± .03	8.05 ± .03	8.41 ± .03
H_2O (formula)[4]	0.992	0.922	0.976	0.985	1.027
			Unit cell parameters		
a (Å)	13.7300(6)	13.7285(9)	13.7357(7)	13.7164(13)	13.7053(3)
V (Å^3)	2588.27(26)	2587.42(50)	2591.51(42)	2580.59(74)	2574.34(17)

[1]The following components were analyzed but not detected: Fe_2O_3, MnO, MgO, BaO, SrO.
[2]Si/Al ratio consistent with EPMA analysis listed.
[3]Range in Si/Al observed in individual spot EPMA analyses.
[4]Number of moles of H_2O in formula unit based on 6 framework oxygens, calculated from H_2O wt% and stoichiometry based on NMR determination of Si/Al.

them. Insufficient quantities of the opaque separate were available to perform NMR characterization on a pure sample; however, this sample was used in the calorimetric and X-ray investigations. Similar material obtained from Ward's was used in the experimental studies of Murphy and others (1996) and Wilkin and Barnes (1998). The sample from the Junnila claim in San Benito County, California (ANA-SBC) is the same as sample ANA003 of Neuhoff and others (2003) and was donated by S. Kleine of Great Basin Minerals. The sample consisted of a small piece of a tectonic inclusion of hydrothermally-altered basalt from a large serpentinite massif containing a vein of analcime and natrolite. The sample was crushed slightly and the analcime hand-picked under a microscope. The sample from Bolzano, Italy (ANA-BZI) had been donated by D. R. Waldbaum and was from the material used by Apps (ms, 1970) in his experimental studies of analcime solubility. The sample was obtained in the form of crushed pure analcime. The last sample from Mt. Vesuvius, Italy (ANA-MVI) was separated from a leucitic tephra. The initial sample was part of a pyroclastic deposit from the Avellino plinian eruption (3550 yr. B.P.), and consists of dark-gray lava clast with phenocrysts of clinopyroxene and minor leucite and olivine in a groundmass that also contains plagioclase and opaques. The analcime consisted of transparent crystals within an amygdule.

Sample Compositions

Direct analyses of anhydrous compositions were performed by electron probe microanalysis (EPMA). These analyses were performed on an automated JEOL 733A electron microprobe at Stanford University operated at 15 kV accelerating potential and 15 nA beam current using natural geologic samples for calibration. Beam width was varied between 10 and 30 μm depending on grain size and raw counts were collected for 20 seconds and converted to oxide weight percents using the CITZAF correction procedure after accounting for unanalyzed oxygen following the methods of Tingle and others (1996). Three to twelve individual points on several grains were analyzed for all samples. In all cases, results of individual spot analyses were consistent with each other, indicating that the samples were homogeneous. Representative single point EPMA results for these samples are listed in table 1; the averages of all points analyzed for an individual sample are similar to the listed spot analyses. It can be seen in table 1 that all four samples are essentially free of extraframework cations other than Na^+. The Si/Al ratios for the samples vary as observed previously in analcime (Passaglia and Sheppard, 2001). Note that the two separates from Mont St. Hilaire have nearly identical compositions. Also listed in table 1 are the ranges in Si/Al observed among various spot analyses.

In order to provide another measurement of the Si/Al ratio and to determine the degree of short-range Si-Al disorder in the samples, ^{29}Si MAS NMR spectra were collected at Stanford University on a modified Varian VXR/Unity-400S spectrometer with a 9.4 Tesla (T) magnet (79.46 MHz for ^{29}Si). Approximately 300 milligrams of each sample were packed into 7 millimeter rotors and spun at 4.7 kHz. Spectra (consisting of 1000 to 10000 transients) were collected using a single 2 microseconds pulse (radio frequency tip angle of $\sim 30°$) using a relaxation delay of 10 seconds. This latter value was chosen to maximize signal to noise in the spectrum. Test spectra collected using longer relaxation delays exhibited identical relative peak intensities, indicating that differential relaxation between the signals was minimal. Spectra and chemical shifts (δ) were referenced to external tetramethyl silane. Peaks in ^{29}Si MAS NMR spectra were fit by least squares regression using the Varian VNMR software package. Errors in the fits are assumed to be on the order of 1 percent of each individual peak area based on repeated fitting of the spectra using different starting values and peak shape models.

TABLE 2

^{29}Si MAS NMR data for analcime

Sample	Site	δ (ppm)	I[1]
ANA-MSHG	Si(4Al)	-86.4	0.011
	Si(3Al)	-91.0	0.145
	Si(2Al)	-96.2	0.637
	Si(1Al)	-101.0	0.195
	Si(0Al)	-106.0	0.011
ANA-SBC	Si(4Al)	-86.9	0.020
	Si(3Al)	-91.2	0.227
	Si(2Al)	-96.4	0.642
	Si(1Al)	-101.3	0.111
ANA-BZI	Si(4Al)	-86.6	0.013
	Si(3Al)	-92.0	0.180
	Si(2Al)	-96.7	0.696
	Si(1Al)	-101.9	0.105
	Si(0Al)	-107.4	0.006
ANA-MVI	Si(4Al)	-85.6	0.012
	Si(3Al)	-91.5	0.124
	Si(2Al)	-96.6	0.582
	Si(1Al)	-101.9	0.257
	Si(0Al)	-107.2	0.025

[1]Relative intensity (peak area)

Results obtained by fitting the ^{29}Si MAS NMR spectra for the samples listed in table 1 are given in table 2 (results for samples ANA-MSHG and ANA-SBC were presented previously by Neuhoff and others, 2003). For every sample except ANA-SBC, five signals are present in the ^{29}Si MAS NMR spectra that correspond to tetrahedrally-coordinated Si with 4 Al, 3 Al + 1 Si, 2Al + 2 Si, 1 Al + 3 Si, and 4 Si second nearest neighbors (for example, Lippmaa and others, 1981; Phillips and Kirkpatrick, 1994; Neuhoff and others, 2003). These signals are hereafter referred to as Si(*n*Al) pentads, where *n* is the number of Al atoms in the second nearest neighbor coordination shell. The Si(0Al) signal is not present in the spectrum for ANA-SBC. The range of δ values obtained for these signals is consistent with previous studies of analcime (Lippmaa and others, 1981; Phillips and Kirkpatrick, 1994; Neuhoff and others, 2003), supporting the assignments listed in table 2. The relative abundances of the Si(*n*Al) signals vary systematically with framework Si/Al ratio in analcime and other highly symmetrical zeolites (Engelhardt and Michel, 1987; Neuhoff and others, 2003) as observed for the more prominent signals listed in table 2. The results in table 2 permit assessment of the Si/Al ratio of the samples via the relationship (Klinowski and others, 1982)

$$\mathrm{Si/Al} = \frac{4}{\sum_{n=1}^{4} n \cdot I_{Si(nAl)}} \qquad (1)$$

where $I_{Si(nAl)}$ is the observed relative intensity of the Si(nAl) line in the ^{29}Si MAS NMR spectrum. Equation (1) assumes complete Al avoidance (that is, the absence of Al-O-Al linkages in the framework; Loewenstein, 1954). The Si/Al ratios calculated via equation (1) for the samples in this study are listed in table 1. While insufficient sample of ANA-MSHO was available to collect a reasonable ^{29}Si MAS NMR spectrum on this material, observations of peak intensities for mixtures of the glassy and opaque portions of the Mont St. Hilaire sample gave essentially identical Si/Al ratios to that obtained for ANA-MSHG.

In all cases, the Si/Al ratio obtained from equation (1) is lower (that is, indicates a more aluminous composition) than those calculated from the EPMA analyses listed in table 1. The cause of this discrepancy is unclear, but is not related to a violation of Al avoidance. If significant Al-O-Al linkages were present, then equation (1) would overestimate the Si/Al ratio, which is the opposite of the phenomenon observed with these samples. In addition, Al-O-Al linkages have been ruled out in one of these samples (ANA-MSHG) by a previous ^{17}O multiple quantum MAS NMR study (Zhao and others, 2001). Previous analyses of the analcimes in our study do not consistently point to either method as being more correct. Analyses of samples from Mont St. Hilaire (also supplied by Ward's Scientific) using inductively coupled plasma emission spectrometry by Murphy and others (1996) and Wilkin and Barnes (1998) indicate compositions of $Na_{1.02}Al_{1.02}Si_{1.98}O_6 \cdot H_2O$ (Si/Al = 1.96) and $Na_{0.99}Al_{0.99}Si_{2.01}O_6 \cdot H_2O$ (Si/Al = 2.02), respectively. These values (particularly that of Murphy and others, 1996) are more consistent with the NMR results than are the EPMA analyses of table 1. A chemical analysis (by unspecified technique) of the analcime from Bolzano, Italy reported in Apps (ms, 1970) corresponds to $Na_{0.93}Al_{0.98}Si_{2.03}O_6 \cdot 0.97H_2O$ (Si/Al = 2.07), more consistent with the EPMA analysis of ANA-BZI in table 1. It should be noted that Si/Al as determined by NMR represents a bulk average, whereas the EPMA analyses are spot analyses. The NMR-based Si/Al ratios are consistent with the water contents of the samples in this study, and in light of the several potential sources of error in EPMA analyses (analysis of non-representative grains, uncertainties in matrix corrections, alkali and water volatilization), the framework compositions of analcime determined by ^{29}Si MAS NMR are used in the analysis of the calorimetric data. Exploratory calculations on the calorimetric data were performed assuming the EPMA-based stoichiometries; these calculations resulted in identical interpretations as to the stoichiometry and enthalpy of mixing in analcime solid solutions.

The weight percent of water in the samples was measured by thermogravimetric analysis (TGA) in a Netzsch STA 449C instrument at the University of Florida by measuring the total weight loss of pre-weighed samples heated to 750°C at 10°C/min in a 65 ml/min stream of ultrapure N_2 gas. Only one weight loss feature was observed in the TGA curves, as noted previously (for example, van Reeuwijk, 1974; Giampaolo and Lombardi, 1994). The weight percent H_2O was taken as the percentage of the initial mass lost over this feature, and is listed in table 1.

Two models have been presented previously of the relationship between framework composition and water content in analcime under standard conditions. Saha (1959) measured the water contents of synthetic analcimes over a wide range in Si/Al and suggested that Si-Al substitution followed a stoichiometry consistent with exchange of one mole of $SiO_2 \cdot 0.5H_2O$ for $NaAlO_2$; that is, the water content of analcime is a function of the framework contents. Some other studies support this conclusion (for example, Wilkinson and Whetten, 1964). However, in his study of the energetics of analcime solid solutions, Wise (1984) suggested that the stoichiometric model proposed by Saha (1959) was not consistent with thermodynamic mixing theory, and indicated that the molar water content of analcime is independent of framework Si/Al, maintaining a constant ratio of 1 mole H_2O per 6 framework oxygens. (This conclu-

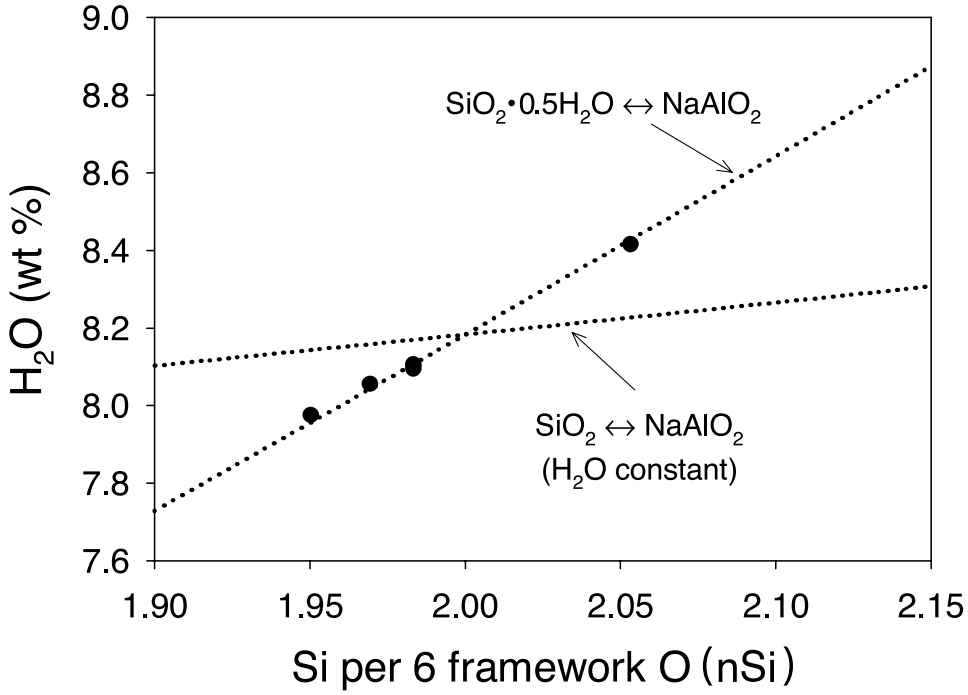

Fig. 1. Weight percent water determined by TGA for the analcime specimens this study (symbols) as a function of the number of moles of Si per 6 framework O (as determined by ^{29}Si MAS NMR). Symbol size corresponds to the uncertainty in the water analyses. The two dotted curves represent previously proposed mixing models for analcime: one in which $SiO_2 \cdot 0.5H_2O$ exchanges for $NaAlO_2$ and another in which the molar water content does not change with substitution of SiO_2 for $NaAlO_2$ (see text).

sion is a consequence of assumptions made by Wise, 1984, concerning the properties of mixing in analcime that are inconsistent with the model described in this study). It should be noted that most analcime samples have compositions close to the stoichiometry $NaAlSi_2O_6 \cdot H_2O$ (a stoichiometry consistent with both models) and the errors in determination of water content in many analyses are large enough to be consistent with either model. The H_2O weight percent values determined in this study are plotted in figure 1 as a function of the Si content. The curves represent the theoretical variation of H_2O weight percent as a function of Si consistent with each of these models. It can be seen that the samples in this study fall directly on the curve that obeys Saha's (1959) model and are inconsistent with the constant-H_2O model. Also note that if the EPMA analyses were used in constructing this plot (instead of the NMR-derived Si/Al), the samples in table 1 would not be consistent with either model. It thus appears that H_2O exchange for Na in the structure of analcime is coupled to Si-Al exchange. This same behavior was observed in other zeolites such as stilbite (Fridriksson and others, 2001). Consequently, the compositions of samples in this study are taken to be:

ANA-MSHG: $(NaAl)_{1.016}Si_{1.984}O_6 \cdot 0.992H_2O$
ANA-MSHO: $(NaAl)_{1.016}Si_{1.984}O_6 \cdot 0.992H_2O$
ANA-SBC: $(NaAl)_{1.049}Si_{1.951}O_6 \cdot 0.976H_2O$
ANA-BZI: $(NaAl)_{1.030}Si_{1.970}O_6 \cdot 0.985H_2O$
ANA-MVI: $(NaAl)_{0.946}Si_{2.054}O_6 \cdot 1.027H_2O$

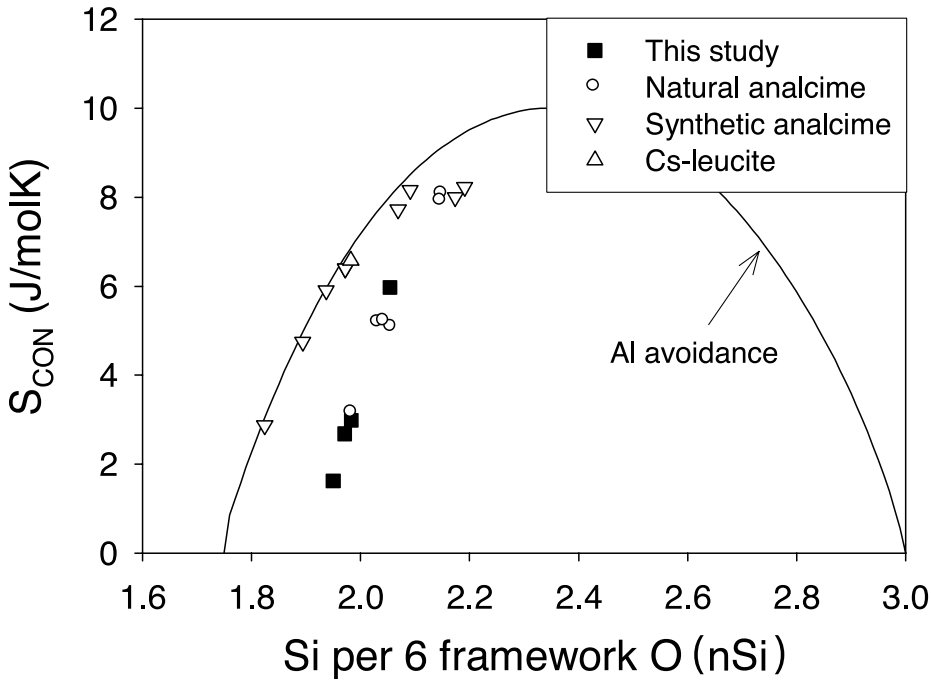

Fig. 2. Configurational entropies (S_{CON}) of natural and synthetic analcimes and Cs-leucite as a function of the number of moles of Si per 6 framework O calculated from ^{29}Si MAS NMR spectra. Data from this study, Murdoch and others (1988), Joshi and others (1991), Phillips and Kirkpatrick (1994), He and others (1995), Herreros and Klinowski (1995), Kato and Hattori (1998), and Takaishi (1998; personal communication from Yamazaki). The curve labeled "Al avoidance" denotes the theoretical compositional dependence of S_{con} in analcime assuming that the only ordering mechanism is complete avoidance of Al-O-Al linkages (see Phillips and Kirkpatrick, 1994).

Unit Cell Measurements

Unit-cell dimensions and volumes were determined at Lafayette College utilizing a Scintag DMS 2000 automated diffractometer. Scans were made from 12° to 102° 2Θ at 0.25°/min in continuous scanning mode utilizing filtered Cu radiation and a monochromator. Cu$K_{\alpha 2}$ peaks were mathematically stripped using Scintag software. Diffraction maxima were determined by Scintag's Peakfinder program. Unit-cell refinements were carried out utilizing the software of Holland and Redfern (1997) from manually corrected $K_{\alpha 1}$ data based on a silicon internal standard (NBS standard reference material 640a having a stated unit-cell dimension of 5.430826 Å). Unit-cell dimensions for all analcime specimens are reported in table 1.

ENTROPIC PROPERTIES OF ANALCIME SOLID SOLUTIONS

Neuhoff and others (2003) recently calculated the configurational entropy (S_{CON}) of a series of analcime samples from ^{29}Si MAS NMR data and used this data to discern the nature of solid solution and Si-Al disorder in analcime. The values of S_{CON} reported by Neuhoff and others (2003) were calculated using the cluster variation method (CVM), which accounts for the probability of next-nearest neighbor (nearest tetrahedral neighbor) configurations among Si and Al (see Kikuchi, 1951; Phillips and Kirkpatrick, 1994; Neuhoff and Stebbins, 2001). These calculations are recast in figure 2 relative to a molar unit containing 6 framework oxygens, as opposed to the unit cell

(96 framework oxygens) used by Neuhoff and others (2003). Also shown in figure 2 are the corresponding calculations for the samples used in this study as well as that reported by Phillips and Kirkpatrick (1994) for a sample of Cs-leucite.

It can be seen in figure 2 that the S_{CON} data define two trends with respect to framework composition: a trend with relatively higher values of S_{CON} for a given composition (that is, more disordered) comprised of synthetic analcimes and Cs-leucite, and a lower trend (that is, more ordered) comprised mostly of natural samples, including those used in this study (see Neuhoff and others, 2003 for details). The two trends appear to reflect two distinct short-range ordering states in analcime, and thus two separate solid solutions. Samples belonging to both of these trends appear to lack long range order, with the more entropic trend corresponding to the maximum Si-Al disorder possible under the constraint of Al avoidance (curve in fig. 2) and the less entropic trend exhibiting greater degrees of short range order consistent with avoidance of Al-O-Si-O-Al linkages (see Neuhoff and others, 2003, for details). In addition to the samples depicted in figure 2, Neuhoff and others (2003) considered a sample described by Kohn and others (1995) that appears to exhibit long range Si-Al ordering, and is thus distinct from the long-range disordered samples considered here. Hereafter, these two trends are referred to as low analcime (more ordered array) and high analcime (more disordered array). These two arrays trend towards a value of $S_{CON} = 0$ (that is, short-range ordered) at a framework composition corresponding to 17 Al in the unit cell for low analcime [corresponding to a molar formula of approximately $(NaAl)_{1.0625}Si_{1.9375}O_6 \cdot 0.969H_2O$] and 20 Al in the unit cell for high analcime [corresponding to a molar formula of $(NaAl)_{1.25}Si_{1.75}O_6 \cdot 0.875H_2O$].

Most natural samples have compositions that lie within the compositional limits of the natural array. Those that do not (that is, those with > 1.063 Al atoms per formula unit) are either long-range ordered (and thus would give a negative S_{CON} as calculated by the CVM; see Neuhoff and Stebbins, 2001) or would potentially have a state of disorder consistent with high analcime. The most Al-rich analcimes are typically found in relatively high-temperature parageneses such as pegmatitic veins around alkaline intrusions (for example, the samples from Mont St. Hilaire in this study) or as phenocrysts of possible primary magmatic origin in silica-deficient volcanic rocks (Passaglia and Sheppard, 2001). An obvious exception to this generalization is represented by sample ANA-SBC, which is clearly formed at temperatures close to surface conditions (Wise and Gill, 1977). Nonetheless, the predominance of Al-rich analcimes in high-temperature parageneses is consistent with higher degrees of disorder than encountered in those formed at lower temperatures.

It is interesting to note that the Si-Al ordering state in high analcime is also seen in other alkali metal-bearing ANA structure materials. The sample labeled Cs leucite in figure 2 (from Phillips and Kirkpatrick, 1994) was a natural (K)leucite that was ion exchanged to the Cs endmember. As noted by Phillips and Kirkpatrick (1994), the ^{29}Si MAS NMR spectrum for this specimen illustrates that leucite only exhibits short-range Si-Al ordering consistent with Al avoidance. Natural Cs-bearing analcimes and pollucite (the Cs analog of leucite and analcime) appear to exhibit similar states of disorder. Teertstra and others (1994) reported ^{29}Si MAS NMR results for several synthetic and natural Cs-bearing analcimes and Na-bearing pollucites (the Cs analog of analcime). Their spectra are relatively poorly resolved, and visual inspection suggests that the reported fits do not account for all peaks in the spectra. Nevertheless, the relative proportions of the peaks that were fit by these authors are consistent with the spectra of materials lying along the high analcime array of figure 2. This fact suggests that the Cs, Na-bearing analcime samples studied by Hovis and others (2002) exhibit short-range Si-Al disorder similar to high analcime.

CALORIMETRY

Calorimetric Methods

The calorimetric system used to measure enthalpies of solution, described by Hovis and Roux (1993) and Hovis and others (1998), is capable of obtaining highly precise data on very small sample sizes. Sample weights for individual calorimetric experiments in the present study ranged from 15 to 103 milligrams. Each sample was dissolved in 910.1 grams (about one liter) of 20.1 weight percent hydrofluoric acid (HF) at 50°C under isoperibolic conditions (meaning that the temperature of the medium surrounding the calorimeter was held constant) utilizing an internal sample container (Waldbaum and Robie, 1970). Either one or two dissolution experiments were performed in each liter of acid. Multiple experiments in the same solution had no detectable effect on the data, because of the high dilution of dissolved ions in the acid. Because the analcime samples dissolved rapidly, the calorimetric experiments were conducted on crushed, but not extremely fine-grained material. This procedure avoided any possibility of heat effects associated with small grain sizes (Nitkiewicz and others, 1983).

Enthalpies of Solution

Calorimetric data for all samples are reported in table 3 and shown in figure 3. In order to gain a sense for calorimetric precision, twice the standard deviation of the enthalpies of solution ($\Delta H_{sol,\ 50°C}$) for all experiments on each sample were computed, and then divided by the average heat of solution for each sample (calculated as the average of heats of solution calculated from the heat capacity before and after dissolution of the sample). Calculated in this way the spread in calorimetric data for each of the various samples ranged from about 0.15 percent to 0.50 percent of the mean heat-of-solution values, and averaged 0.26 percent among all samples (note that the average error is greatly accentuated by the relatively large error for sample ANA-MSHG, for which very small sample masses were used). This average error constitutes a high degree of calorimetric precision that enabled the detection of energy differences associated with variations in both composition and Si-Al disorder among the samples. As seen in figure 2, with the exception of ANA-MSHO, $\Delta H_{sol,\ 50°C}$ increases somewhat (that is, becomes less negative) with increased Si content for the samples. The heat of solution measured for ANA-MSHO is clearly more negative than that of the isochemical sample ANA-MSHG.

Enthalpies of Formation

It is possible to calculate the enthalpies of formation from the elements (ΔH_f) for all analcime samples using the following reaction scheme:

$$\underset{\text{albite}}{xNaAlSi_3O_8} + [(1.5\text{-}x)/2]H_2O_{(liquid)} = \underset{\text{analcime}}{(NaAl)_xSi_{3\text{-}x}O_6 \cdot [(1.5\text{-}x)/2]H_2O} + \underset{\text{quartz}}{(3\text{-}4x)SiO_2} \quad (2)$$

In this formulation "x" represents the number of moles of NaAl per 6 framework oxygens. Recalling that $\Delta H_{sol,\ 50°C}$ and ΔH_f are related to one another as

$$\sum \Delta H_{sol,50°C}(\text{reactants}) - \sum \Delta H_{sol,50°C}(\text{products}) = \sum \Delta H_{f,50°C}(\text{products}) - \sum \Delta H_{f,50°C}(\text{reactants}), \quad (3)$$

ΔH_f for analcime is the only unknown quantity in the formulation. Because the temperature of the calorimetric measurements (50°C) differs from the reference temperature for most compilations of thermodynamic data (25°C), the enthalpies of formation must be adjusted to account for the difference in heat content between

TABLE 3

Calorimetric data

Sample	Run Number	Gram formula mass of sample[1] (g/mol)	Sample mass (g)	Temperature increase during dissolution (°C)	C_p before[2] (J/°C)	C_p after[3] (J/°C)	ΔH_{sol} before[4] (kJ/mol)	ΔH_{sol} after[5] (kJ/mol)
ANA-MSHG	1014	220.3600	0.02008	0.011674	3866.23	3865.39	-494.31	-494.20
	1017	220.3600	0.01991	0.011476	3868.36	3869.36	-490.34	-490.47
	1019	220.3600	0.01936	0.011112	3868.15	3868.28	-488.26	-488.28
							AVERAGE[6]	*-490.98 ± 2.72*
ANA-MSHO	1015	220.3600	0.01994	0.011595	3868.36	3868.90	-494.93	-495.00
	1016[7]	220.3600	0.01924	0.011275	3865.64	3866.43	-498.18	-498.28
	1018[7]	220.3600	0.01484	0.008694	3865.35	3865.51	-498.02	-498.05
							AVERAGE[6]	*-497.08 ± 1.64*
ANA-SBC	1007	220.7850	0.01713	0.009869	3872.63	3870.33	-491.62	-491.34
	1008	220.7850	0.01630	0.009389	3871.87	3866.73	-491.42	-490.76
							AVERAGE[6]	*-491.28 ± 0.37*
ANA-BZI	844[7]	220.5403	0.10098	0.058234	3869.61	3870.83	-491.17	-491.34
	974[7]	220.5403	0.09977	0.057656	3868.61	3866.98	-492.05	-491.86
							AVERAGE[6]	*-491.60 ± 0.42*
ANA-MVI	979	219.4586	0.07459	0.042957	3872.29	3869.15	-488.44	-488.04
	980[7]	219.4586	0.07450	0.043024	3868.69	3866.81	-489.32	-489.09
							AVERAGE[6]	*-488.72 ± 0.59*

[1]Based on formula unit compositions listed in text (based on Si/Al from ^{29}Si MAS NMR data).
[2]Calorimeter heat capacity before dissolution.
[3]Calorimeter heat capacity after dissolution.
[4]Enthalpy of solution at 50 °C based on heat capacity before dissolution.
[5]Enthalpy of solution at 50 °C based on heat capacity after dissolution.
[6]Average of all ΔH_{sol} before and ΔH_{sol} after values for a given sample.
[7]Dissolution run in acid of preceding calorimetric experiment.

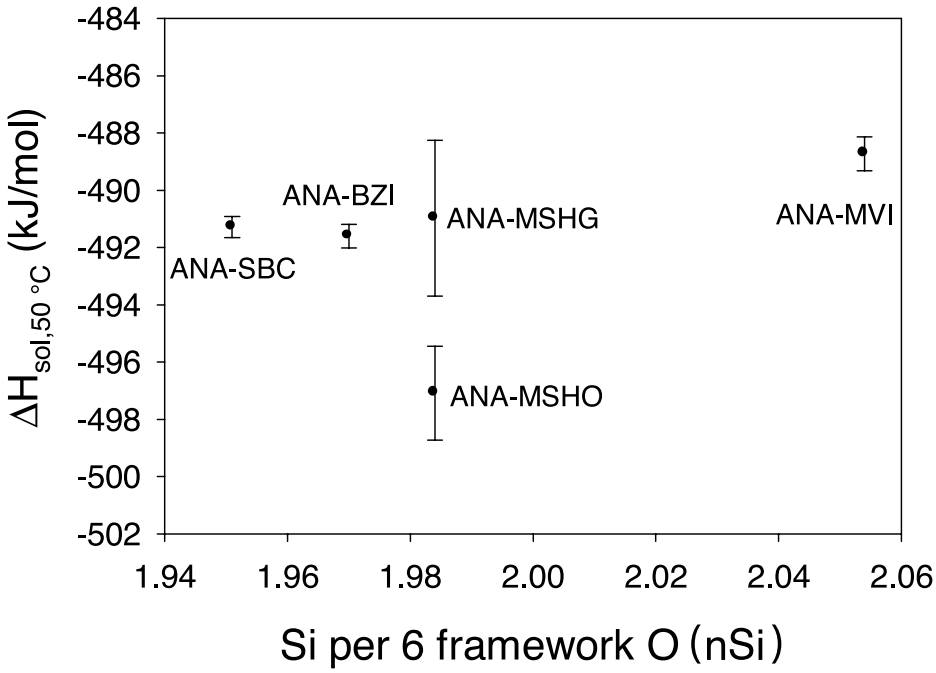

Fig. 3. Enthalpies of solution of analcime in HF at 50°C determined in this study (table 3) as a function of the number of moles of Si per 6 framework O.

these temperatures. Calculation of "true" ΔH_f from the elements at 50°C for analcime can then be calculated from the "true" ΔH_f of albite, quartz and water given by

$$\Delta H_{f,50^\circ C} = \Delta H_{f,25^\circ C} + \int_{298.15}^{323.15} C_{p,substance} dT - \sum \int_{298.15}^{323.15} C_{p,elements} dT \qquad (4)$$

where C_p is the heat capacity, the integrals represents the change in heat content of the minerals from 298.15 K (25 °C) to 323.15 K (50 °C) of the substance (that is, albite, quartz, water or the elements), and the summation is over the constituent elements of the substance in question in their respective proportions. The "apparent" ΔH_f (compare Benson, 1968; Helgeson and others, 1978) at 50°C is given by

$$\Delta H_{f,50^\circ C} = \Delta H_{f,25^\circ C} + \int_{298.15}^{323.15} C_{p,substance} dT. \qquad (5)$$

Enthalpies of formation at 25°C of low albite (−3935.0 kJ/mol), water (−285.83 kJ/mol), and quartz (−910.7 kJ/mol) from Robie and Hemingway (1995) were used in conjunction with the enthalpies of solution at 50°C of low albite (−627.34 kJ/mol, Hovis, 1988), water (−0.19 kJ/mol, Hovis, unpublished data), quartz (−137.36 kJ/mol, Hovis, 1982) and analcime (this investigation) to determine the "true" and apparent ΔH_f for analcime at 50°C. Heat capacity equations for evaluation of the integrals in equations (4) and (5) for albite, quartz, Al, Si, O_2 and H_2 were taken from Robie and Hemingway (1995), that for water was calculated using the computer code SUPCRT92 (Johnson and others, 1992), and that for Na were taken from Kubas-

chewski and others (1993). The resulting enthalpies of formation at 50°C for analcime, albite, quartz and water are listed in table 4.

The enthalpy of formation of analcime at 25°C can be calculated by rearrangement of equation (4) or (5) provided that the integral representing the heat content of analcime over the interval from 25°C to 50°C can be evaluated. Johnson and others (1982) determined the heat contents of an analcime of composition $(NaAl)_{0.96}Si_{2.04}O_6 \cdot 2.02H_2O$ (note that the water content was adjusted from their reported composition, within the errors in their chemical analysis, to comply with the stoichiometry of analcime solid solutions discussed above) from which the temperature dependence of C_p can be evaluated. Although the heat capacity of analcime is likely to vary somewhat with composition, data are not currently available to assess the magnitude of this phenomenon. Estimates of the consequences of the compositional dependence of C_p on the integrals in equations (4) and (5) were made using two models. In the first model, C_p as a function of temperature was adjusted to account for the molecular weight differences along the solid solution (by back-calculating the specific heat, assuming that it is independent of composition, and then calculating the heat capacity). The second model assumed that the change in C_p is negligible across a balanced chemical reaction between Johnson and others' (1982) analcime, an analcime with the composition of interest, and the oxides (using C_p for water in analcime as determined by Johnson and others, 1982, and the properties of the oxides from Robie and Hemingway, 1995; compare Neuhoff, ms, 2000). With both models, the heat content of analcime between 25° and 50°C varies by less than 50 J/mol over the range of composition of the samples in this study; that is, this variation is less than the precision of the ΔH_f determinations. Consequently, the same value of the integral of $(C_p\, dT)$ between 25° and 50°C (5.4 kJ/mol) was used for each of the samples in this study to calculate the ΔH_f at 25°C from equation (4). These values are also listed in table 4, along with previous determinations of ΔH_f at 25°C (Barany, 1962; Johnson and others, 1982; Ogorodova and others, 1996). These latter values have been adjusted from the published values within their respective thermochemical cycles to account for differences in the previously assumed water content of analcime and the water content consistent with the present solid solution model for analcime. In all cases, the molar water stoichiometry listed in table 4 for samples from the literature is within error of the reported chemical analyses. Also listed in table 4 are ΔH_f calculations based on the extrapolation of ΔH_{sol} data for solid solutions between analcime and Rb- and Cs-leucite from Hovis and others (2002).

The enthalpy of formation data at 25°C in table 4 are presented in figure 4. It can be seen in figure 4 that the data appear to define two trends, both exhibiting a linear dependence of $\Delta H_{f,25}$ on the number of moles of Si. The less stable (that is, less negative) trend is comprised of sample ANA-MSHO along with those of Hovis and others (2002) and Ogorodova and others (1996). The more stable trend includes all other samples from this study as well as those studied by Johnson and others (1982) and Barany (1962). Weighted linear regression of the data along the less stable trend gives

$$\Delta H_{f,25}(\text{kJ/mol}) = -3669.3(75.6) + \text{nSi} \times 183.0(37.6) \quad (6)$$

and along the more stable trend gives

$$\Delta H_{f,25}(\text{kJ/mol}) = -3692.5(35.7) + \text{nSi} \times 191.4(17.8) \quad (7)$$

where the numbers in parentheses are the standard errors. The relatively large magnitude of the errors reflects in large part the uncertainties in the data points; simple linear regression of these data result in nearly identical equations with standard errors considerably smaller than indicated in equations (6) and (7).

TABLE 4

Thermodynamic properties used in thermochemical cycles and calculated enthalpies of formation for analcime

Sample	Composition	$\Delta H_{sol,50\ °C}$ (kJ/mol)	$H_{50\ °C} - H_{25\ °C}$[1] (kJ/mol)	"true"[2] $\Delta H_{f,\ 50\ °C}$ (kJ/mol)	Apparent[3] $\Delta H_{f,\ 50\ °C}$ (kJ/mol)	$\Delta H_{f,\ 25\ °C}$ (kJ/mol)
			analcime			
ANA-MSHG[4]	$(NaAl)_{1.016}Si_{1.984}O_6 \cdot 0.992H_2O$	-490.98 ± 2.72[4]	5.4[13]	-3312.6 ± 4.0[17]	-3306.9 ± 4.0[17]	-3312.3 ± 4.0[17]
ANA-MSHO[4]	$(NaAl)_{1.016}Si_{1.984}O_6 \cdot 0.992H_2O$	-498.02 ± 1.64[4]	5.4[13]	-3306.5 ± 3.3[17]	-3300.8 ± 3.3[17]	-3306.2 ± 3.3[17]
ANA-SBC[4]	$(NaAl)_{1.049}Si_{1.951}O_6 \cdot 0.976H_2O$	-491.28 ± 0.37[4]	5.4[13]	-3319.8 ± 3.1[17]	-3314.1 ± 3.1[17]	-3319.5 ± 3.1[17]
ANA-BZI[4]	$(NaAl)_{1.030}Si_{1.970}O_6 \cdot 0.985H_2O$	-491.60 ± 0.42[4]	5.4[13]	-3315.2 ± 3.0[17]	-3309.5 ± 3.0[17]	-3314.9 ± 3.0[17]
ANA-MVI[4]	$(NaAl)_{0.946}Si_{2.054}O_6 \cdot 1.027H_2O$	-488.72 ± 0.59[4]	5.4[13]	-3298.9 ± 2.7[17]	-3293.3 ± 2.7[17]	-3298.7 ± 2.7[17]
Analcime[5]	$(NaAl)Si_2O_6 \cdot H_2O$	-496.50 ± 0.21[5]	5.4[13]	-3303.4 ± 2.9[17]	-3297.8 ± 2.9[17]	-3303.2 ± 2.9[17]
Analcime[6]	$(NaAl)_{0.96}Si_{2.04}O_6 \cdot 1.02H_2O$[9]	-	5.4[13]	-3303.5 ± 2.6[17]	-3297.9 ± 2.6[17]	-3303.3 ± 2.6[18]
Analcime[7]	$(NaAl)_{0.96}Si_{2.04}O_6 \cdot 1.02H_2O$[9]	-	5.4[13]	-3302.0 ± 3.3[17]	-3296.4 ± 3.3[17]	-3301.8 ± 3.3[19]
Analcime[8]	$(NaAl)_{0.95}Si_{2.05}O_6 \cdot 1.025H_2O$[9]	-	5.4[13]	-3294.3 ± 3.4[17]	-3288.7 ± 3.4[17]	-3294.1 ± 3.4[20]
			Supporting data for thermochemical cycles			
Albite	$NaAlSi_3O_8$	-627.34 ± 0.44[10]	5.3[14]	-3935.5 ± 2.6[17]	-3929.8 ± 2.6[17]	-3935.0 ± 2.6[21]
Quartz	SiO_2	-137.36 ± 0.35[11]	1.1[14]	-910.8 ± 1.0[17]	-909.6 ± 1.0[17]	-910.7 ± 1.0[21]
Water	H_2O	-0.19 ± 0.01[12]	1.9[15]	-285.0 ± 0.1[17]	-283.9 ± 0.1[17]	-285.8 ± 0.1[21]
Na metal	Na	-	0.72[16]	-	-	-
Al metal	Al	-	0.61[14]	-	-	-
Si Metal	Si	-	0.51[14]	-	-	-
H gas	H_2	-	0.72[14]	-	-	-
O gas	O_2	-	0.73[14]	-	-	-

[1] $\int_{298.15}^{323.15} C_{p,substance} dT$. [2]Enthalpy of formation from the elements; includes $H_{50\ °C}$–$H_{25\ °C}$ for the elements. [3]Apparent enthalpy of formation from the elements (cf. Benson, 1968; Helgeson and others, 1978). [4]This study (average values from table 3). [5]Extrapolated results for analcime endmember of Rb- and Cs-leucite solid solutions from Hovis and others (2002). [6]Analcime sample from Table Mountain, Colorado (USA) reported by Barany (1962). [7]Sample from Skookumchuck Dam, Washington (USA) reported by Johnson and others (1982). [8]Sample from Nidym River, Siberia reported by Ogorodova and others (1996). [9]Composition adjusted from that assumed in original study to agree with stoichiometry of solid solution in analcime adopted in this study. All adjustments were within error of original analysis. [10]Hovis (1988). [11]Hovis (1982). [12]Hovis (unpublished results). [13]Calculated from temperature dependence of heat capacity data presented by Johnson and others (1982); see text. [14]Calculated from heat capacity equations in Robie and Hemingway (1995). [15]Calculated using the computer code SUPCRT92 (Johnson and others, 1992). [16]Calculated from heat capacity equations in Kubaschewski and others (1993). [17]Calculated from equations (3-5) in text. [18]Calculated from revised data of Barany (1962) and thermochemical cycles presented by Johnson and others (1982) for composition in second column. [19]Calculated from data and thermochemical cycles presented by Johnson and others (1982) for composition in second column. [20]Calculated from data and thermochemical cycles presented by Ogordova and others (1996) for composition in second column. [21]Robie and Hemingway (1995).

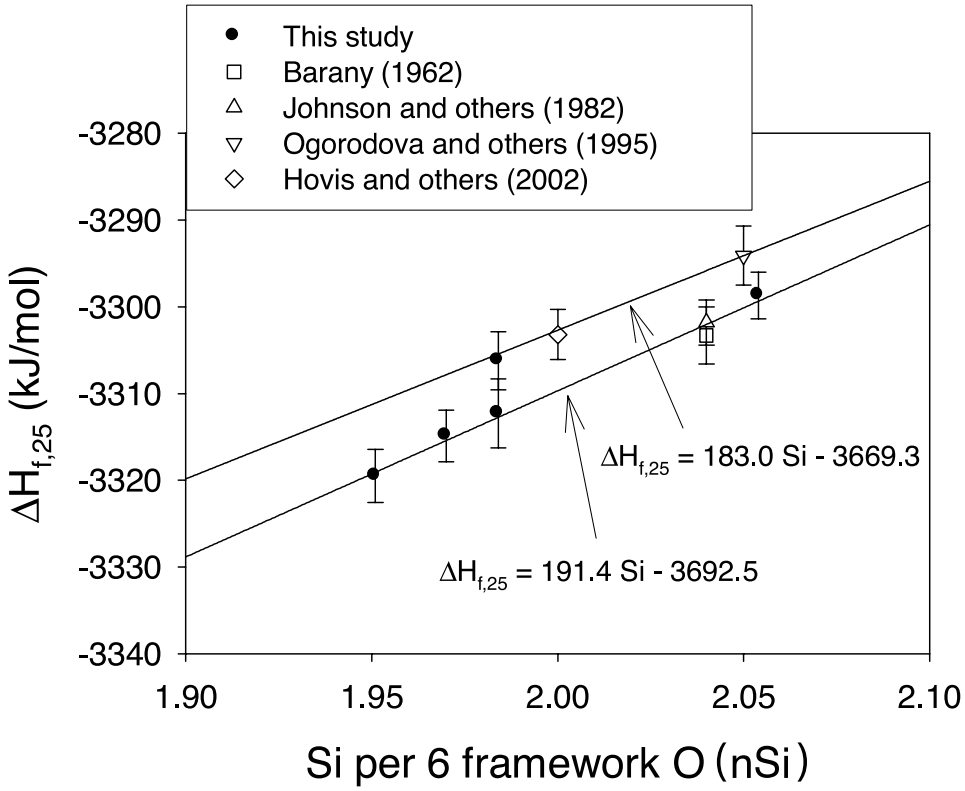

Fig. 4. Enthalpy of formation at 25°C of analcime as a function of the number of moles of Si per 6 framework O (symbols). The lines represent weighted least squares linear regressions (eqs 6 and 7; see text) of the trends for low (more stable trend) and high analcime (less stable trend).

The two trends apparent in figure 4 likely reflect different short-range Si-Al ordering states in analcime, and we propose that they represent low analcime (more stable trend) and high analcime (less stable trend). With the exception of the datum from Johnson and others (1982), for which NMR data are unavailable, all of the samples defining the more stable trend in figure 4 are part of the low analcime array of samples in figure 2. Unfortunately, data are not available to assess the ordering sate of the samples defining the less stable trend in figure 4. However, based on the arguments presented above about pollucite, it seems likely that the extrapolated datum from Hovis and others (2002) is a member of the high analcime array in figure 2. While we were unable to acquire a usable ^{29}Si MAS NMR spectrum on ANA-MSHO, it appears based on the thermodynamic properties retrieved below for a sample from Mont St. Hilaire studied by Murphy and others (1996) that some samples from this locality are high analcime. The sample used by Ogorodova and others (1996) originated from the Nidym River region of Siberia. Few details about the paragenesis of this sample are available, but it almost certainly is an alteration product of the Siberian Trap lavas exposed in the locality (which might imply a relatively low-temperature origin). Interpretation of this datum is hampered by experimental difficulties associated with the lead borate drop solution calorimetric technique used by Ogorodova and others (1996). This technique can be plagued by uncertainties in the final states of calorimetric experiments involving hydrous phases such as analcime (Navrotsky and others,

TABLE 5

Partial molar enthalpies of formation of components in analcime solid solutions

	$\Delta \overline{H}_f$ (kJ/mol)	
Solution	$SiO_2 \cdot 0.5H_2O$	$NaAlO_2$
Low analcime	-1039.8 ± 5.9	-1230.1 ± 11.9
High analcime	-1040.1 ± 12.2	-1223.1 ± 24.9

1994). However, given the fact that it is essentially co-linear with the Hovis and others (2002) and ANA-MSHO data, it is tentatively assigned to high analcime. The difference between the two trends at a given composition then defines the enthalpy of disordering from low to high analcime. The magnitude of this heat effect (~6 kJ/mol of analcime) is consistent with disordering enthalpies in feldspars on a per mol oxygen basis (compare Hovis, 1988).

The linearity of both trends in figure 4 indicates that these solid solutions exhibit negligible enthalpies of mixing (H^{EX}) over the range of composition that was studied, implying that these solutions are athermal. Linear dependence of $\Delta H_{f,25}$ on composition for Si-Al substitution in zeolites appears to be relatively common (for example, Petrovic and Navrotsky, 1997; Shim and others, 1999). In the case of faujasite (Petrovic and others, 1993; Petrovic and Navrotsky, 1997; Yang and Navrotsky, 2000), which was studied over the widest range of Si-Al substitution of any zeolite system, $\Delta H_{f,25}$ is a linear function of composition from aluminum mole fractions (X_{Al}) of 0 to ~ 0.45. Athermal behavior in faujasite appears to hold over a wide range of temperature as well, from 25° to 700°C (Neuhoff and Stebbins, 2001). Although the results of figure 4 only establish athermal behavior over the composition range of nSi = ~1.95 to ~2.05, it seems likely based on the behavior of other zeolites that $\Delta H_{f,25}$ is a linear function of composition over the more limited range of Si-Al substitution (nSi = ~1.8 to ~2.22) observed in analcime. This behavior is assumed in the rest of the calculations presented below.

The partial molar enthalpies of formation ($\Delta \bar{H}_f$) of components in analcime solid solutions were regressed from the data in table 4 assuming athermal behavior of both the more stable and less stable trends in figure 4. Although the thermodynamic properties for analcime solid solutions are calculated at the end of the paper for mineral end-members, these solutions can be viewed as mixtures of the components $SiO_2 \cdot 0.5H_2O$ and $NaAlO_2$. The data in table 4 were adjusted to correspond to molar formulas containing one mole of $SiO_2 \cdot 0.5H_2O$ and $NaAlO_2$ for the purposes of weighted linear regression of $\Delta \bar{H}_f$ of the complementary component. The results of these regressions are presented in table 5 for high and low analcime solid solutions, where it can be seen that $\Delta \bar{H}_f$ of $SiO_2 \cdot 0.5H_2O$ and $NaAlO_2$ are related to the coefficients in equations (6) and (7) by a factor of three (the difference in the molar size of species in the two analyses). Given the relatively large errors in these regressions, $\Delta \bar{H}_f$ for $SiO_2 \cdot 0.5H_2O$ and for $NaAlO_2$ are similar between these solutions. The partial molar enthalpy of $SiO_2 \cdot 0.5H_2O$ for both solutions is less stable than the $\Delta H_{f,25}$ of quartz + 0.5 water (−1053.6 kJ/mol; Robie and Hemingway, 1995) which is consistent with the absence of pure silica analcime in nature. Furthermore, $\Delta \bar{H}_f$ for $SiO_2 \cdot 0.5H_2O$ in both solutions agrees very well with $\Delta H_{f,25}$ for pure silica zeolites (−896.6 to −908.3 kJ/mol; Petrovic and others, 1993) plus 0.5 $\Delta H_{f,25}$ for liquid water.

Exploratory calculations were performed assuming that the water content of analcime does not vary with Si-Al substitution (see above). Enthalpies of formation were computed as above for the samples in this study assuming a stoichiometry of 1

mole of H_2O per six framework oxygens, and the resultant values used to assess the $\Delta\bar{H}_f$ for the components $SiO_2 \cdot 0.3333H_2O$ and $NaAlO_2 \cdot 0.3333H_2O$. These calculations led to $\Delta\bar{H}_f$ of $SiO_2 \cdot 0.3333H_2O$ that was ~ 20 kJ/mol more stable than $\Delta H_{f,25}$ of quartz + 0.33333 water, which implies that hypothetical pure silica analcime would be stable with respect to quartz and all other silica polymorphs in the presence of water. Thus, the improbable energetic consequences of assuming that the water content of analcime is not a function of Si-Al substitution appear to bolster the substitutional model adopted above in which the water content of analcime increases with increasing Si.

MIXING PROPERTIES IN ANALCIME SOLID SOLUTIONS

As noted above, analcime exhibits solid solution both among Si and Al in its tetrahedral framework and with respect to extraframework cations and water. This discussion ignores solid solutions involving water site vacancies (that is, the effects of reversible dehydration) and substitution of Ca^{+2}, Cs^+, Rb^+, K^+ and other cations for Na^+ in the extraframework sites. Thus, the only solution considered is the coupled substitution of $NaAlO_2$ for $SiO_2 \cdot 0.5H_2O$ presented above, which describes the composition of most naturally occurring analcime samples (Passaglia and Sheppard, 2001).

In contrast to other highly symmetrical zeolites (such as those with the FAU, LTA, and CHA framework types; see Meier and others, 2001) which exhibit framework Al mole fractions from ~0 to 0.5, analcime exhibits a relatively restricted degree of Si-Al substitution in natural and synthetic systems. The most aluminous analcimes known have framework contents corresponding to 1.2 Al atoms per 6 framework oxygens (Saha, 1959; Wilkinson and Whetten, 1964; Wilkinson and Hensel, 1994; Passaglia and Sheppard, 2001); these samples are either synthetic or probable primary phenocryst phases in igneous rocks. The most siliceous analcimes known in both synthetic and natural systems have compositions approaching 2.25 Si atoms per 6 framework oxygens (Saha, 1959; Broxton and others, 1987). From figure 2, it appears that the extent of Si-Al substitution may be substantially larger for high analcime than low analcime, provided that synthetic samples are considered. Aluminum contents in high analcime are the most aluminous analcimes known, and the most siliceous analcimes ever synthesized (Saha, 1959; under conditions that likely form metastable high analcime) have Si contents approaching 2.25 Si per 6 framework oxygens. In contrast, low analcime, which includes all low-temperature analcimes studied by ^{29}Si MAS NMR, is restricted to framework Al contents < ~1.06 (Neuhoff and others, 2003). Based on the similar genetic conditions of the samples analyzed by Broxton and others (1987) from Yucca Mountain, Nevada (USA) to those of the most siliceous natural samples in figure 2, it appears that the low analcime solution may also have an upper compositional bound of 2.25 Si per six framework oxygens (as proposed by Saha, 1959).

The following sections present retrievals of the properties of mixing for low analcime solid solutions. The siliceous endmember for this solution is taken as $(NaAl)_{0.75}Si_{2.25}O_6 \cdot 1.125H_2O$ for reasons presented above. Sample ANA-SBC appears to be the most Al-rich natural analcime aside from those in high-temperature parageneses, and its approximate composition $[(NaAl)_{1.05}Si_{1.95}O_6 \cdot 0.975H_2O]$ is taken as the aluminous endmember in this solution. Although hypothetical endmembers suggested by Neuhoff and others (2003) would be equally plausible, the endmember compositions chosen here encompass the range of observed low-temperature analcime compositions and permit retrieval of endmember thermodynamic properties with considerably less extrapolation from existing data.

Volumes of Mixing

Figure 5 shows reported values of the *a* cell parameter and equivalent molar volume (V) of the analcime samples in this study along with the numerous samples

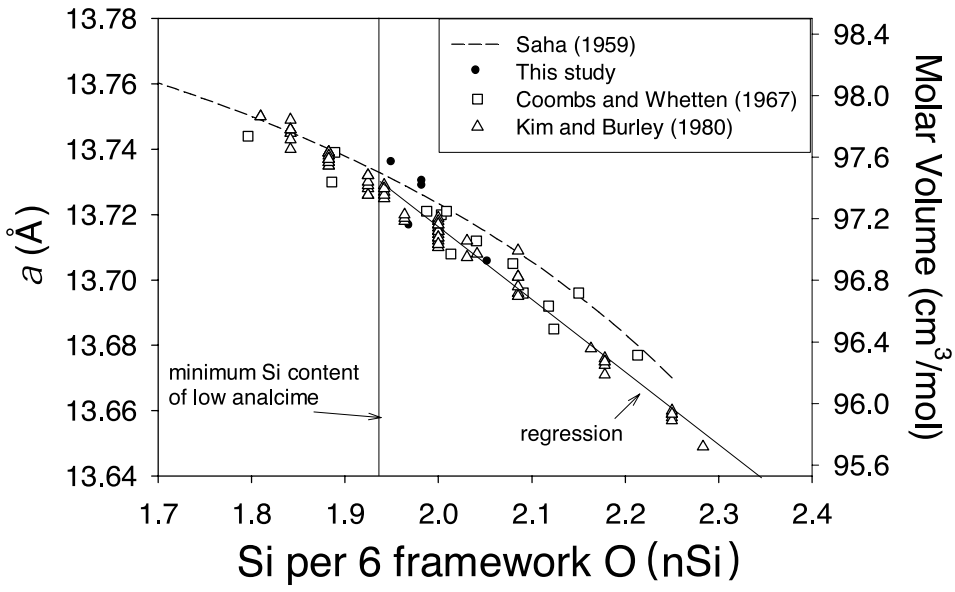

Fig. 5. The *a* unit cell parameter and the molar volume of analcime as a function of the number of moles of Si per 6 framework O (symbols). The vertical line marks the minimum Si content possible in low analcime (Neuhoff and others, 2003). The curve labeled Saha (1959) represents the relationship between *a* and framework composition proposed by that author. The line labeled regression represents the least squares linear regression of the low analcime data in the figure (eq 8; see text).

from the literature, as well as the determinative curve proposed by Saha (1959). It can be seen that, taken as a whole, the data plotted in figure 5 define a distinct, but somewhat noisy, trend indicating that V is inversely related to Si content. It is unclear whether the variation of V reported for a given Si content (or vice versa) reflects measurement errors and uncertainties, or actual inter-sample differences. It seems likely that both play a role. Segregation between synthetic samples (for example, the run products of Kim and Burley, 1980) and natural samples (those of this study and the compilation of Coombs and Whetten, 1967) is not readily apparent. It appears from this observation that there may be little volumetric consequence to the difference in ordering state exhibited by the two arrays of figure 2.

The scatter in the data of figure 5 precludes unambiguous assessment of the excess volume of mixing (V^{EX}) in low analcime solid solutions. While the determinative curve proposed by Saha (1959) suggests that V of analcime is not linearly related to the molar framework content, this curve does not appear to be the best representation of the data in figure 5. Coombs and Whetten (1967) proposed a roughly similar dependence, although the position of their hand-drawn curve was more consistent with the data in figure 5. Visual inspection of figure 5 suggests that a slight curvature is present in the data when taken as a whole. However, when the data on the siliceous side of the minimum possible Si content in low analcime (Neuhoff and others, 2003; vertical line in fig. 5) are considered separately, the data appear to define a linear trend. The trend suggests a small, if not negligible V^{EX} for this solid solution, although the scatter of the data in figure 5 do not preclude a finite value of V^{EX}. In the absence of compelling evidence for non-ideality in the volumes of mixing in low analcime solutions, the data with Si >1.94 in figure 5 was fit to the linear equation

$$V\ (cm^3/mol) = -4.68(0.13)Si + 106.48(0.26) \quad (8)$$

which is shown by the solid line labeled "regression". The molar volumes of low analcime endmembers and intermediate compositions listed in table 6 were calculated from equation (8).

Entropies of Mixing

The S_{CON} data in figure 2 can be used to assess the excess entropy of mixing (S^{EX}) in analcime solid solutions (Neuhoff and Stebbins, 2001; Neuhoff and others, 2003). Assuming the absence of an excess calorimetric contribution to the entropy of these zeolites (which seems reasonable given the general success of oxide summation algorithms for predicting S in zeolites of variable composition; Neuhoff, ms, 2000), the difference between the measured S_{CON} and that for ideal mixing ($S_{CON,ideal}$) represents S^{EX} in solid solutions with ordered endmembers (compare Neuhoff and Stebbins, 2001):

$$S^{EX} = S_{CON} - S_{CON,ideal} \tag{9}$$

Because of the choice of endmembers in this study, for which S_{CON} is not equal to zero, an alternative expression for S^{EX} was derived from the data of figure 2.

When the low analcime data of figure 2 are recast in terms of the mol fractions of the aluminous and siliceous endmembers ($X_{aluminous}$ and $X_{siliceous.}$, respectively; fig. 6), they can be represented by the relationship

$$S_{CON} = X_{aluminous}S_{CON,aluminous} + X_{siliceous}S_{CON,siliceous} + W(X_{aluminous}\ \ln X_{aluminous} + X_{siliceous}\ \ln X_{siliceous}). \tag{10}$$

where W is an empirical fitting parameter and the mol fractions of the aluminous and siliceous endmembers are given by

$$X_{aluminous} = 1 - X_{siliceous} = (nAl - 0.75)/0.75. \tag{11}$$

The data in figure 6 were fit to equation (10) to give W = -2.20 ± 0.75 J/molK, $S_{CON,alum}$ = 1.54 ± 0.24 J/molK, and $S_{CON,siliceous}$ = 9.22 ± 0.83 J/molK. The rightmost term in equation (10) is analogous to the role of S_{CON} in equation (9) and corresponds to the deviation between the experimentally determined S_{CON} and that of a mechanical mixture of the endmembers characterized by $S_{CON,aluminous}$ and $S_{CON,siliceous}$ (given by the sum of the first two terms on the left hand side of eq 10). This quantity is related to S^{EX} for the solid solution by

$$S^{EX} = W(X_{aluminous}\ \ln X_{aluminous} + X_{siliceous}\ \ln X_{siliceous}) - S_{CON,ideal}. \tag{12}$$

where $S_{CON,ideal}$ is given by

$$S_{CON,ideal} = -3R\Sigma_k X_k\ \ln X_k \tag{13}$$

in which the subscripts k denote the endmembers in the solid solution and the number three corresponds to the number of tetrahedral sites in the molar formula. Note that the excess entropy is negative. Combining equations (12) and (13) leads to:

$$S^{EX} = (W + 3R)(\Sigma_k X_k\ \ln X_k). \tag{14}$$

Gibbs Energies of Mixing and Activity Composition Relationships

The excess Gibbs energy of mixing (G^{EX}) for a solution can be calculated from

$$G^{EX} = H^{EX} - TS^{EX}. \tag{15}$$

As noted above, H^{EX} appears to be negligible in analcime solid solutions. Thus, combining equations (14) and (15) leads to

TABLE 6

Summary of molar heat capacities, entropies, and volumes of analcime

Study	Composition[1]	C_p coefficients ($C_p = a + bT + cT^{-2}$) a (J/molK)	b (J/molK^2)	c (JK/mol)	$S_{0\rightarrow298.15}$[5] (J/molK)	V_{298}[6] (cm^3/mol)
		Calorimetric data[4]				
Johnson and others (1982)	$(NaAl)_{0.96}Si_{2.04}O_6 \cdot 1.02H_2O$	108.77	0.29689	1341599	227.15	96.95
		Endmembers				
	$(NaAl)_{1.05}Si_{1.95}O_6 \cdot 0.975H_2O$	115.87	0.28741	1028130	226.62	97.37
	$(NaAl)_{0.75}Si_{2.25}O_6 \cdot 1.125H_2O$	92.19	0.31901	2073027	228.37	95.96
		Experimental Samples				
Hemley (1973)[2]	$(NaAl)_{0.96}Si_{2.04}O_6 \cdot 1.02H_2O$	108.77	0.29689	1341599	227.15	96.95
Apps (ms, 1970)	$(NaAl)_{1.030}Si_{1.970}O_6 \cdot 0.985H_2O$[3]	114.29	0.28951	1097790	226.74	97.27
Redkin and Hemley (2000)	$(NaAl)_{1.05}Si_{1.95}O_6 \cdot 0.975H_2O$	115.87	0.28741	1028130	226.62	97.37
Murphy and others (1996)	$(NaAl)_{1.02}Si_{1.98}O_6 \cdot 0.99H_2O$	113.50	0.29057	1132620	226.79	97.23
Wilkin and Barnes (1998)	$(NaAl)_{0.99}Si_{2.01}O_6 \cdot 1.005H_2O$	111.13	0.29373	1237110	226.97	97.09

[1]Compositions adjusted for water stoichiometry. [2]See text for data source. [3]Sample used by Apps (ms, 1970) was same as sample ANA-BZI in this study. [4]Recalculated from adiabatic and drop calorimetric results of Johnson and others (1982). [5]Estimated value; retrieved values shown in table 7 used in calculations (see text). [6]Calculated from equation 8.

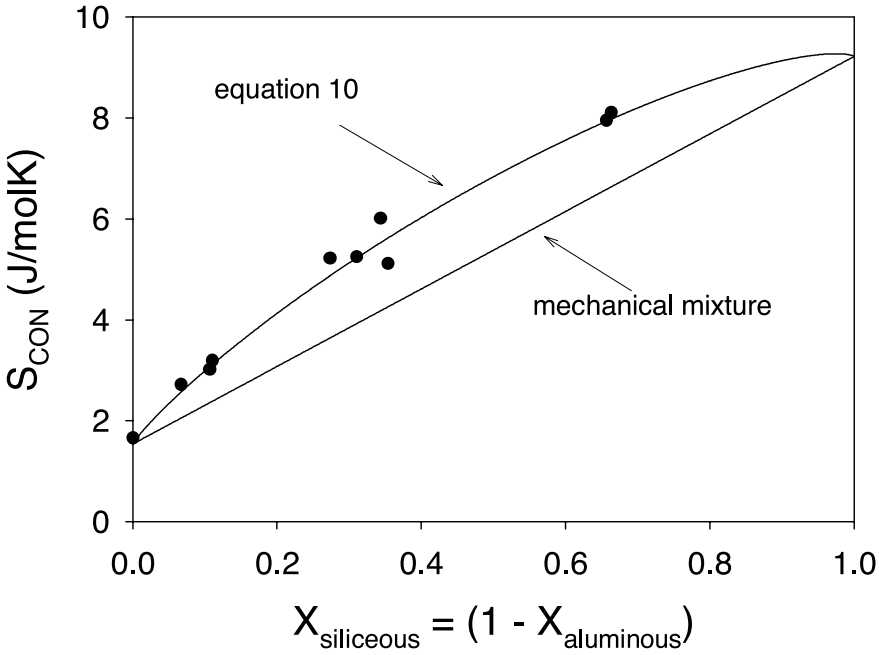

Fig. 6. Configurational entropies of low analcime (fig. 2) as a function of the mol fraction of the siliceous analcime endmember. The curve labeled mechanical mixture is a linear trend between the configurational entropies of the siliceous and aluminous low analcime endmembers. The trend labeled equation 10 represents the fit to equation10 discussed in the text.

$$G^{EX} = -T(W + 3R)(\Sigma_k X_k \ln X_k). \tag{16}$$

The activities of the endmembers in these solid solutions are given by

$$a_k = (X_k)^n \gamma_k \tag{17}$$

where γ_k is the activity coefficient and the exponent, n, accounts for the stoichiometry of tetrahedral sites. The activity coefficients can be assessed through the equations above by noting that

$$RT \ln \gamma_k = G^{EX} - (1 - X_k)(\partial G^{EX}/\partial(1 - X_k))_{T,P,X_k} \tag{18}$$

where the right hand side is an expression of the partial molar Gibbs energy of mixing of endmember k. Combination of equations (16) and (18) leads to an explicit expression for γ_k:

$$\ln \gamma_k = -(W/R + 3) \ln (X_k) \tag{19}$$

which can be combined with equation (17) to give the explicit expression for the activity of an endmember in the low analcime solid solution

$$a_k = (X_k)^{(-W/R)}. \tag{20}$$

As a consequence of the athermal nature of low analcime solid solution, γ_k is not a function of temperature. Figure 7 illustrates the relationship between X_k and a_k computed from equation (20), along with the same relationship for ideal solutions in which a_k is equal to the cube of X_k. The strongly non-ideal nature of this solution is

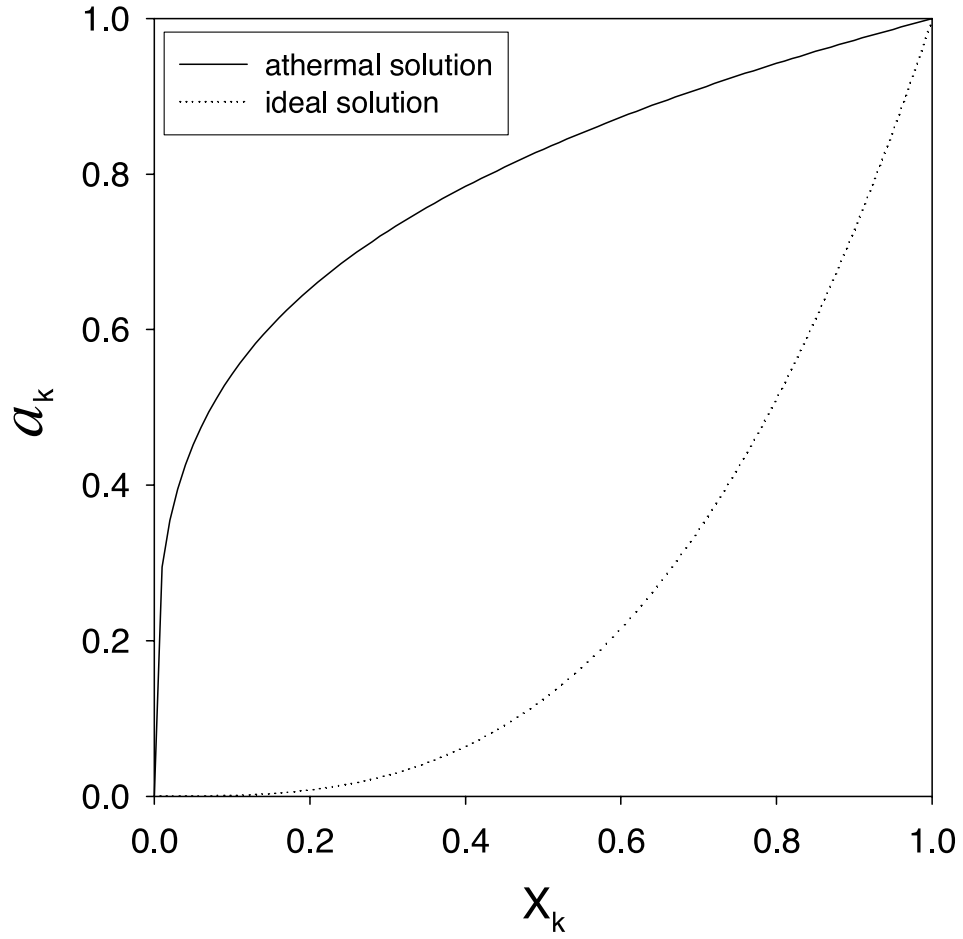

Fig. 7. Relationship between the mol fraction of an endmember in the low analcime solid solution (X_k) and the activity of the endmember (a_k) for the athermal solid solution model proposed in the text (solid curve) and an ideal solid solution model (dashed curve).

evident in figure 7 by the difference between the curves for the two activity models. It can also be seen in the figure that a_k approaches X_k as the composition approaches the endmembers.

THERMODYNAMIC PROPERTIES OF LOW ANALCIME SOLID SOLUTIONS

The solid solution model presented above was used to derive thermodynamic properties for the aluminous and siliceous endmember compositions from published observations of equilibria involving low analcime, aqueous electrolyte solutions, and albite. The procedures and thermodynamic formulations followed in these calculations were essentially those of Helgeson and others (1978). Thermodynamic data for albite, water, and aqueous species were calculated with the SUPCRT92 computer program (Johnson and others, 1992). Calculations involving albite were conducted using thermodynamic data for low albite unless otherwise noted. The following calculations assume that analcime is fully hydrated. Calculations of the hydration state of analcime, as a function of temperature and pressure by Neuhoff and others (2000),

indicate that analcime was fully hydrated under the conditions of the hydrothermal experiments considered in this study.

Entropy, Heat Capacity, and Volume of Analcime

The entropy at elevated temperatures and pressures ($S_{T,P}$) of analcime was represented by the relation

$$S_{T,P} = S_{0\rightarrow 298.15} + S_{CON} + \int_{298.15}^{T} \frac{C_p}{T}\, dT \qquad (21)$$

assuming that thermal expansion is negligible (see below), where $S_{0\rightarrow 298.15}$ is the relative entropy change from 0 to 298.15 K (the "Third Law" entropy), and C_p is the molar, constant pressure heat capacity. The temperature dependence of C_p was represented by the Maier and Kelley (1932) polynomial

$$C_p = a + bT + cT^{-2} \qquad (22)$$

where a, b, and c are empirical fitting coefficients. The only calorimetric observations of $S_{0\rightarrow 298.15}$ and C_p of analcime are those of Johnson and others (1982) and Barany (1962) which were conducted on samples with a composition of $(NaAl)_{0.96}Si_{2.04}O_6 \cdot 1.02H_2O$. The observations of Johnson and others (1982) presented in table 6 are generally consistent with those of Barany (1962) and cover a much larger temperature range. In order to estimate the effect of compositional variation in low analcime solid solutions on C_p and $S_{0\rightarrow 298.15}$, an oxide summation algorithm (Helgeson and others, 1978; Ransom and Helgeson, 1994; Neuhoff, ms, 2000) was employed in which the change in C_p (and the coefficients a, b, and c in eq 22) and $S_{0\rightarrow 298.15}$ was assumed to be negligible across a balanced chemical reaction between the analcime studied by Johnson and others (1982) and that with the composition of interest. Oxide properties were taken from Helgeson and others (1978) except for H_2O. The latter values were taken from Neuhoff (ms, 2000), who calculated C_p and $S_{0\rightarrow 298.15}$ for H_2O ($C_p = -60.37 + 0.1743\ T + 4510000\ T^{-2}$ J/mol and $S_{0\rightarrow 298.15} = 55.02$ J/molK) in analcime from the difference between the calorimetrically determined C_p and $S_{0\rightarrow 298.15}$ for fully hydrated and dehydrated analcime reported by Johnson and others (1982) and Barany (1962). The results of these calculations are listed in table 6 for low analcime endmembers as well as for analcimes with compositions corresponding to those employed in hydrothermal experiments considered in this study. Note that the values of $S_{0\rightarrow 298.15}$ calculated using the oxide summation algorithm (table 6) were slightly adjusted below to afford better correspondence with experimental observations of equilibria involving analcime (see table 7).

The molar volumes of low analcime at 298.15 K, 1 bar ($V_{298.15}$) listed in table 6 were calculated from equation (8). Although V for most rock forming silicates is relatively insensitive to changes in temperature and pressure (for example, Helgeson and others, 1978), this is not the case for analcime. The magnitude (or even the sign) of thermal expansion coefficients in hydrated analcime has not been directly measured over a range of temperature sufficient to assess the energetic consequences of this phenomenon. Cruciani and Gualtieri (1999) measured unit cell parameters of an analcime sample over a wide range of temperature, but calculation of thermal expansion coefficients from their results is hampered by a competing and dramatic change in unit cell size associated with progressive dehydration of their specimen with increasing temperature. The dehydrated analcime resulting from this process clearly exhibits negative thermal expansion from 750 K (the point at which dehydration was complete) to ~950 K (the highest temperature in their study). Little change in cell size was observed in the fully hydrated analcime at temperatures from 298 K to 400 K. From

TABLE 7

Summary of Gibbs energies of formation, enthalpies of formation, and entropies of analcime retrieved from experimental equilibrium observations

Study	Composition[1]	$X_{alum.}$	$X_{silic.}$	$a_{alum.}$	$a_{silic.}$	ΔG_f° (kJ/mol)	ΔH_f° (kJ/mol)	$S_{0\rightarrow298.15}^\circ$ (J/molK)	S_{CON}° (J/molK)	$S_{298.15}^\circ$ (J/molK)
				Endmembers						
	$(NaAl)_{1.05}Si_{1.95}O_6 \cdot 0.975H_2O$	1	0	1	0	-3097.959	-3317.277	225.44	1.54	226.98
	$(NaAl)_{0.75}Si_{2.25}O_6 \cdot 1.125H_2O$	0	1	0	1	-3044.461	-3264.289	232.80	9.22	242.02
				Experimental Samples						
Hemley (1973)[2]	$(NaAl)_{0.96}Si_{2.04}O_6 \cdot 1.02H_2O$	0.7	0.3	0.9097	0.7367	-3082.9 ± 0.2	-3301.8 ± 0.2	228.47	5.13	233.60
Apps (ms)	$(NaAl)_{1.030}Si_{1.970}O_6 \cdot 0.985H_2O$	0.933	0.067	0.9819	0.4877	-3096.4 ± 1.7	-3315.5 ± 1.7	226.12	2.57	228.68
Redkin and Hemley (2000)	$(NaAl)_{1.05}Si_{1.95}O_6 \cdot 0.975H_2O$	1	0	1	0	-3097.0 ± 2.1	-3316.3 ± 2.1	225.44	1.54	226.98
Murphy and others (1996)	$(NaAl)_{1.02}Si_{1.98}O_6 \cdot 0.99H_2O$	0.9	0.1	0.9725	0.5431	-3087.1 ± 0.1	-	226.45	2.99	229.44
Wilkin and Barnes (1998)	$(NaAl)_{0.99}Si_{2.01}O_6 \cdot 1.005H_2O$	0.8	0.2	0.9426	0.6526	-3089.0 ± 1.7	-3308.0 ± 1.7	227.46	4.13	231.59

[1]Compositions adjusted for water stoichiometry; see footnotes to table 6 for additional details.
[2]See text for data source.

this latter observation, and in the absence of other measurements, it is assumed that the thermal expansivity of hydrated analcime is negligible. This assumption likely has relatively little affect on the calculations below, as thermal expansion in tectosilicates is generally less than one percent of total volume up to temperatures of 400°C (the highest temperature considered in this study; Helgeson and others, 1978). In contrast, copious data are available for assessing the extent of isothermal compression in analcime. Unit cell measurements of analcimes at elevated pressures at 298.15 K (Yoder and Weir, 1960; Ott and others, 1986) indicate an apparent volume compression of ~1.5 percent at 5 kb, considerably larger than other rock-forming silicates. It should be noted that some variation in compressibility is observed between analcime samples; the cause of this variation is unclear. Some analcime samples also exhibit phase transitions at elevated pressures (Yoder and Weir, 1960); however, these transitions occur beyond the stability field of analcime. While the retrieval calculations (based on experimental equilibria observed at pressure of 1 kbar or less) are not appreciably affected by changes in V of analcime with pressure, the calculations of univariant phase equilibria presented below are sensitive to this effect. Consequently, the molar volume of analcime at elevated pressures, V_P, as well as the consequent integrals of V with pressure, were calculated from the relationship

$$V_P = V_{298.15} - 0.0000036V_{298.15}(P - 1) \tag{23}$$

where the coefficient in the rightmost term corresponds to the average partial derivative of the molar volume of analcime with respect to pressure at constant temperature calculated from the observations of Ott and others (1986) and Yoder and Weir (1960).

Retrieval of the Standard Gibbs Energies and Enthalpies of Formation of Analcime

The thermodynamic properties of the endmembers in the low analcime solid solution were retrieved from experimental observations of equilibria between analcime, albite and aqueous solutions corresponding to the reactions

$$\underset{\text{analcime}}{(NaAl)_xSi_{3-x}O_6 \cdot [(3\text{-}x)/2]H_2O} = xNa^+ + xAlO_2^- + (3\text{-}x)SiO_{2,aq} + [(3\text{-}x)/2]H_2O \tag{24}$$

and

$$\underset{\text{albite}}{xNaAlSi_3O_8} + [(3\text{-}x)/2]H_2O = \underset{\text{analcime}}{(NaAl)_xSi_{3-x}O_6 \cdot [(3\text{-}x)/2]H_2O} + (4x\text{-}3)SiO_{2,aq} \; . \tag{25}$$

Reaction (24) corresponds to total hydrolysis of analcime, which was experimentally investigated by, Apps (ms, 1970), Murphy and others (1996), and Wilkin and Barnes (1998) for analcime samples of different compositions. Equilibria pertaining to reaction (25) are reported by Apps (ms, 1970), Redkin and Hemley (2000), and Hemley (1973; personal communication to Helgeson and others, 1978; the data were subsequently tabulated by Johnson and others, 1982). Activities of the ions for analcime hydrolysis experiments (reaction 24) were calculated by speciation of reported fluid compositions with the computer code EQ3/6 (Wolery and Daveler, 1992); pH at elevated temperatures was calculated with the EQ6 module by first speciating the fluids at 298.15 K, 1 bar, in EQ3NR and then repeating the speciation calculation on the fluids at the temperature of interest. Two sets of retrieval calculations were

performed: one in which a standard state of unit activity of analcime with compositions corresponding to those in the experiments cited above was adopted, and a second in which the standard state properties of the low analcime endmembers were retrieved (assuming unit activity of the pure endmembers and the activity-composition relations derived above).

In the first set of retrieval calculations, the standard molal Gibbs energies and enthalpies of formation from the elements, ΔG_f° and ΔH_f°, respectively, of the analcimes used in the experiments considered in this study were retrieved from experimental equilibrium observations using the values of V_{298} and C_p coefficients listed in table 6 and values of the entropy at 298.15K, 1 bar ($S_{298.15}$) listed in table 7, which were retrieved from experimental observations of analcime equilibria. The values of ΔG_f° and ΔH_f° retrieved from these calculations are listed in table 7. The errors reported are based on the experimental ranges in the activities of aqueous species in the individual experiments.

The properties of the aluminous low analcime endmember was retrieved from experimental observations of the analog of reaction (25):

$$\underset{\text{albite}}{1.05\ NaAlSi_3O_8} + 0.975\ H_2O = \underset{\text{aluminous low analcime}}{(NaAl)_{1.05}Si_{1.95}O_6 \cdot 0.975H_2O} + 1.2SiO_{2,aq} \quad (26)$$

for which the mass action expression (assuming unit activity of pure water) is

$$\log K = \log a_{\text{aluminous}} + 1.2 \log a_{SiO_{2(aq)}}. \quad (27)$$

Activities of the aluminous and siliceous low analcime endmembers in the experimental analcime samples are listed in table 7. It should be noted that reactions (25) and (26) pertain to metastable equilibria. Because solid solution in low analcime essentially involves an exchange of $SiO_2 \cdot 0.5H_2O$ for $NaAlO_2$, and in the case of the experimental observations considered in these calculations the chemical potential of H_2O is fixed in equilibrium with liquid water, the equilibrium composition of analcime at any given temperature and pressure is solely a function of the chemical potential of SiO_2, in accordance with the reaction

$$\underset{\text{aluminous low analcime}}{0.75(NaAl)_{1.05}Si_{1.95}O_6 \cdot 0.975H_2O)} + 0.9SiO_{2(aq)} + 0.45H_2O = 1.05\ \underset{\text{siliceous low analcime}}{(NaAl)_{0.75}Si_{2.25}O_6 \cdot 1.125H_2O} \quad (28)$$

for which the mass action expression can be expressed as

$$\log K = 1.05 \log a_{\text{siliceous}} - 0.75 \log a_{\text{aluminous}} - 0.9 \log a_{SiO_{2(aq)}}. \quad (29)$$

The phase assemblage albite-analcime-fluid in the experiments of Apps (ms, 1970), Hemley (1973, personal communication to Helgeson and others, 1978), and Redkin and Hemley (2000) can be described by three thermodynamic components (for example, $NaAlO_2$, SiO_2, and H_2O). Phase rule analysis indicates that this assemblage is divariant; thus at the fixed temperature and pressure conditions of the experiments the chemical potentials of the components (including SiO_2) are also constrained. This constraint implies that stable coexistence of analcime of fixed composition with albite and an aqueous solution can only occur at one temperature and pressure. As a consequence, the experimental observations of Apps (ms, 1970), Hemley (1973, personal communication to Helgeson and others, 1978), and Redkin and Hemley

(2000) either pertain to equilibrium between albite, aqueous solutions, and analcime samples whose compositions varied with the conditions of the experiments, or represent metastable equilibrium of compositionally invariant analcime. Lacking experimental observations necessary to assess the degree of re-equilibration of analcime with albite and aqueous solutions as a function of temperature and pressure, it was assumed that the aluminous low analcime endmember was in metastable equilibrium with albite and the fluids in these experiments.

The results of these retrieval calculations are listed in table 7 and shown in figure 8, which compares the experimental observations of log $a_{SiO_{2(aq)}}$ in metastable equilibrium with albite and analcime with that calculated using the thermodynamic properties of albite, H_2O, $SiO_{2(aq)}$ from SUPCRT92 and the properties of aluminous low analcime in tables 6 and 7. In order to maximize agreement between experimental observations over the whole range of temperature of the experimental observations in figure 8, it was necessary to decrease the entropy of aluminous low analcime by ~0.5 percent from that estimated using the oxide summation algorithm; the value of $S_{298.15}^{\circ}$ listed in table 7 was retrieved from experimental equilibrium observations, and $S_{0\rightarrow298.15}$ calculated from the relationship

$$S_{298.15} = S_{0\rightarrow298.15} + S_{CON} \tag{30}$$

where S_{CON} corresponds to that calculated from the regression of equation (10) to the data in figure 6. It can be seen in figures 8A and 8B that there is close agreement between the thermodynamic properties for aluminous low analcime listed in tables 6 and 7 and the experimental observations of Hemley (1973, personal communication to Helgeson and others, 1978) and Redkin and Hemley (2000), respectively. Agreement is generally close for most of the observations of Apps (ms, 1970), although the curve in figure 8C suggests that aluminous low analcime is somewhat more stable than indicated by the measured silica activities at 175° and 200°C. The 200°C datum in figure 8C cannot be reconciled with the 200°C, 1 kbar datum of Hemley (1973, personal communication to Helgeson and others, 1978) and the molar volume of analcime, and given the internal consistency of the other observations in figure 8, this discrepancy was ignored in the retrieval.

The properties of siliceous low analcime were retrieved from experimental observations of reaction (24) by assuming equilibrium with respect to reaction (28) from the experimental observations of Wilkin and Barnes (1998) and Apps (ms, 1970). Attempts were made to include the observations of Murphy and others (1996); however, the observations noted below indicate that the sample used in their study exhibits a greater degree of Si-Al disorder than those used in other studies under consideration. Only the data for the sample from Mont St. Hilaire studied by Wilkin and Barnes (1998) were used in the retrieval calculations. Their experiments on a relatively Si-rich analcime from Wikieup, Arizona (USA) were conducted in a silica glass tube, which provided a secondary buffer for the chemical potential of SiO_2. Comparison of the compositions of fluids reportedly in equilibrium with the Wikieup sample with the solubility of amorphous silica and the results of the current study indicates that the solutions in these experiments did not equilibrate with either analcime or silica glass. Figure 9 depicts activities of $SiO_{2(aq)}$ in aqueous solutions equilibrated with analcime by Apps (ms, 1970) and Wilkin and Barnes (1998). Note that the solubility of analcime in Wilkin and Barnes' (1998) experiments at temperatures of 90°C and above was approached both from under and supersaturation; all other data depicted in figure 9 pertain to solutions that were initially undersaturated with respect to analcime. The curves in figure 9 were generated from the retrieved and estimated thermodynamic data for aluminous and siliceous low analcime (tables 6 and 7) and the thermodynamic properties of aqueous silica and H_2O calculated with

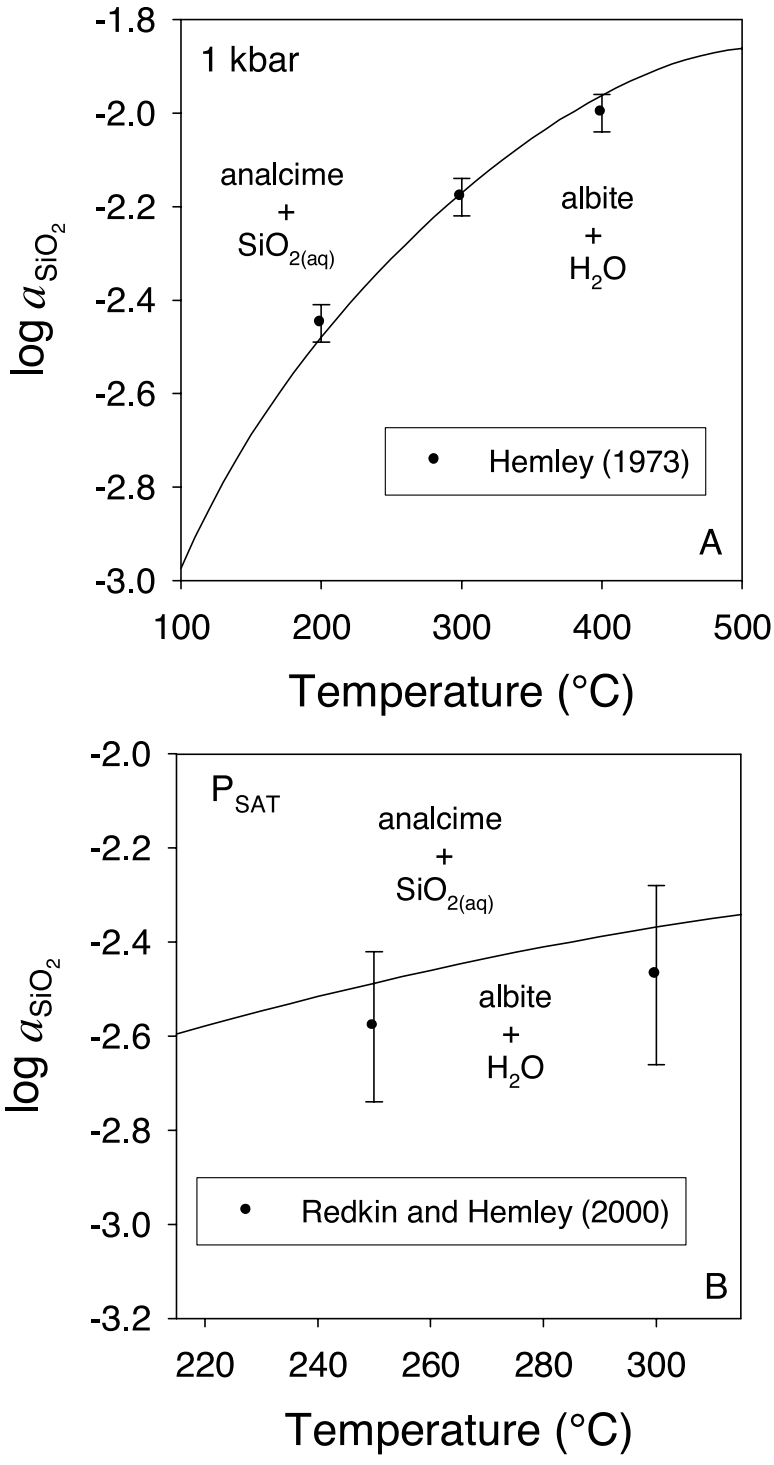

Fig. 8. Experimental observations (symbols) of the activity of aqueous silica in metastable equilibrium with analcime and albite (reaction 25) as a function of temperature at 1 kbar from Hemley (1973, personal communication to Helgeson and others, 1978, A), at pressures corresponding to liquid-vapor equilibrium for water from Redkin and Hemley (2000; B) and Apps (ms, 1970; C). The curves in each panel are consistent with the compositions of analcime in each study and the thermodynamic data for aluminous analcime listed in tables 6 and 7.

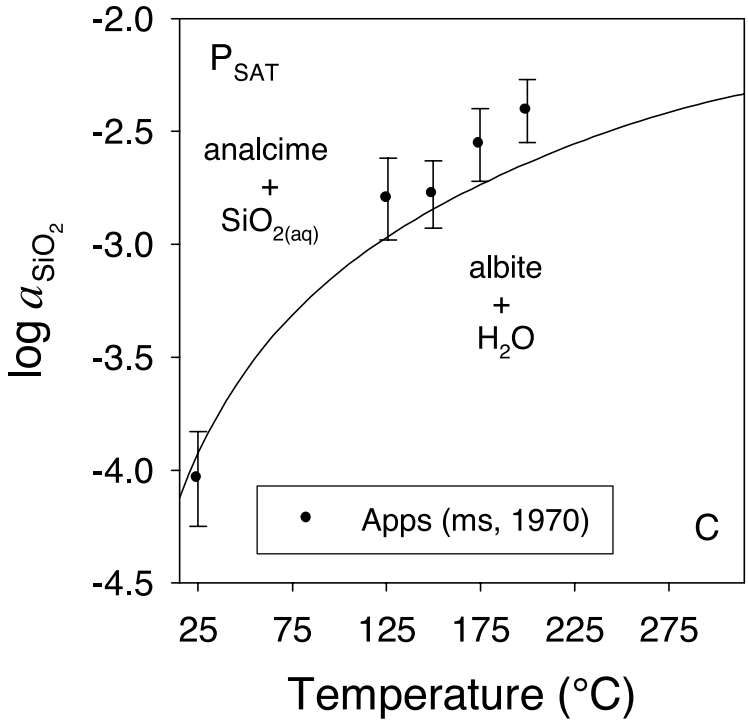

Fig. 8. (continued).

SUPCRT92. It can be seen that the curves in figure 9 are consistent with the data of Apps (ms, 1970) and the observations of Wilkin and Barnes (1998) at temperatures of 90°C and higher. The entropy of siliceous low analcime at 298.15 K, 1 bar was adjusted in the retrieval calculation over that consistent with the estimated value in table 6 in order to reconcile the thermodynamic properties of siliceous low analcime with the temperature distribution of the data in figure 9. This adjustment corresponded to a ~1.7 percent increase in the $S_{0\rightarrow298.15}$ of siliceous low analcime. The values of $S_{0\rightarrow298.15}$ retrieved for aluminous and siliceous low analcime were then used to estimate $S_{0\rightarrow298.15}$ for the experimental analcime compositions in table 7 by assuming no excess calorimetric entropy of mixing in the solid solution.

Figures 10 and 11 compare the solubilities of aluminous and siliceous low analcime calculated from the thermodynamic properties in tables 6 and 7 with the experimental observations of Apps (ms, 1970) and Wilkin and Barnes (1998). The data plotted in figures 10 and 11 correspond to the ion activity products for aluminous and siliceous low analcime hydrolysis (reaction 24)

$$\log Q_{\text{aluminous}} = 1.05 \log a_{Na^+} + 1.05 \log a_{AlO_2^-} + 1.95 \log a_{SiO_{2(aq)}} \qquad (31)$$

and

$$\log Q_{\text{siliceous}} = 0.75 \log a_{Na^+} + 0.75 \log a_{AlO_2^-} + 2.25 \log a_{SiO_{2(aq)}} \qquad (32)$$

calculated from the experimental observations of Apps (ms, 1970) and Wilkin and Barnes (1998). The curves represent the difference between the logarithms of the equilibrium constant for the aluminous and siliceous low analcime analogs of reaction

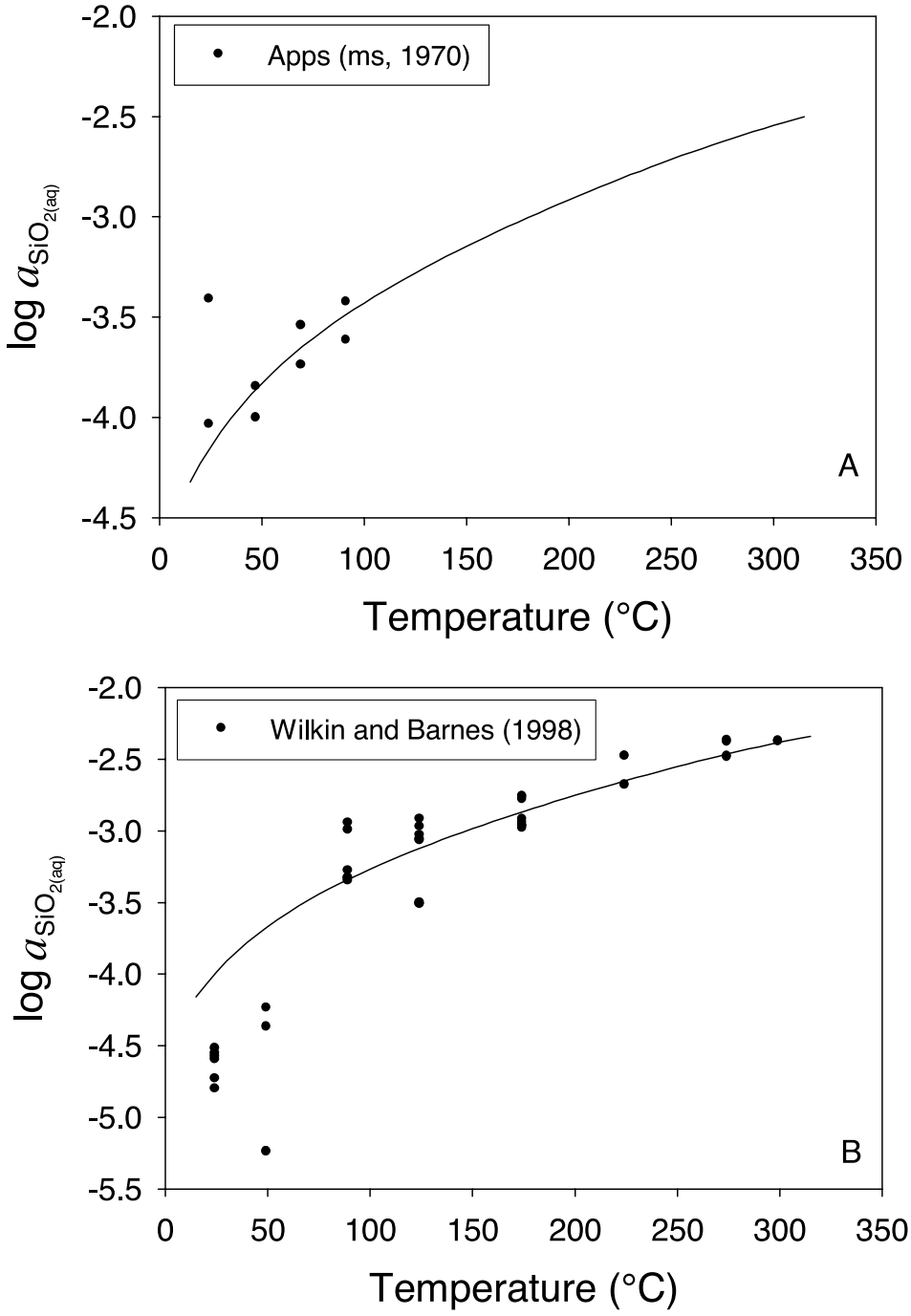

Fig. 9. Experimental observations (symbols) of the activity of aqueous silica in equilibrium with analcime (reaction 27) as a function of temperature at pressures corresponding to liquid-vapor equilibrium for water from Apps (ms, 1970; A) and Wilkin and Barnes (1998; B). The curves in each panel are consistent with the compositions of analcime in each study and the thermodynamic data for aluminous and siliceous analcime listed in tables 6 and 7.

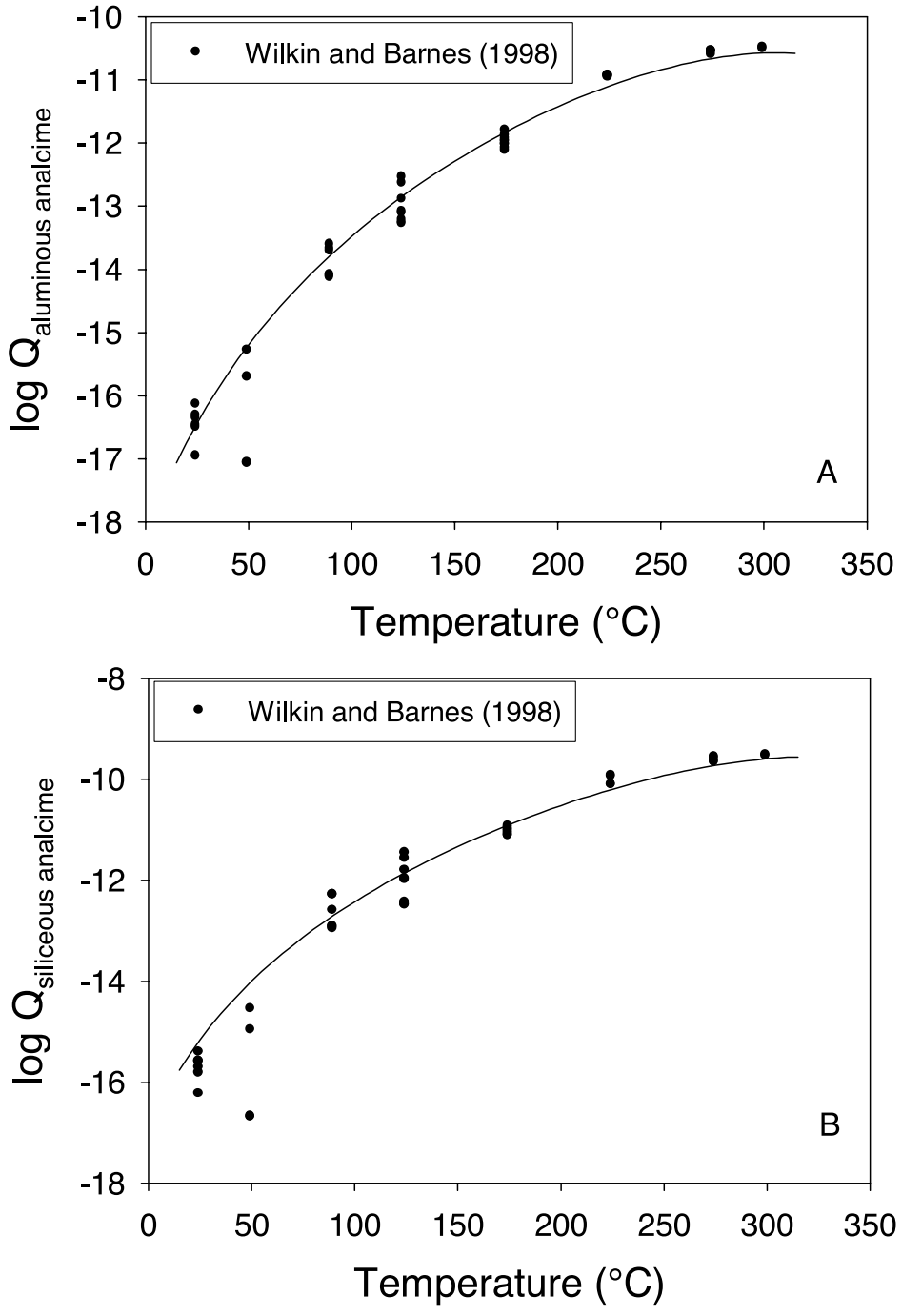

Fig. 10. Experimental determinations (symbols) of the solubility product of aluminous (A) and siliceous (B) analcime as a function of temperature at pressures corresponding to liquid-vapor equilibrium for water from Wilkin and Barnes (1998). The curves in each panel are consistent with the composition of analcime used by Wilkin and Barnes (1998) and the thermodynamic data for aluminous and siliceous analcime listed in tables 6 and 7.

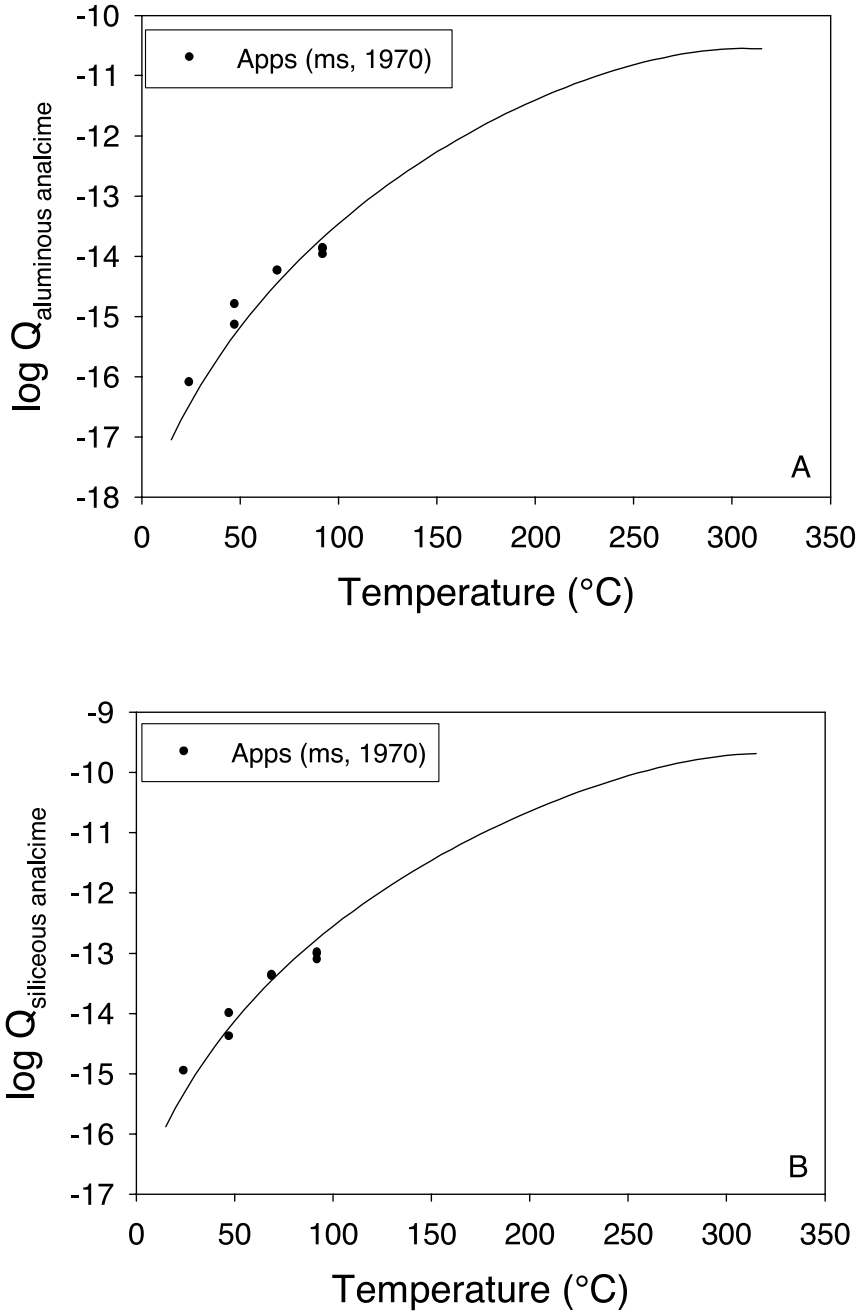

Fig. 11. Experimental determinations (symbols) of the solubility product of aluminous (A) and siliceous (B) analcime as a function of temperature at pressures corresponding to liquid-vapor equilibrium for water from Apps (ms, 1970). The curves in each panel are consistent with the composition of analcime used by Apps (ms, 1970) and the thermodynamic data for aluminous and siliceous analcime listed in tables 6 and 7.

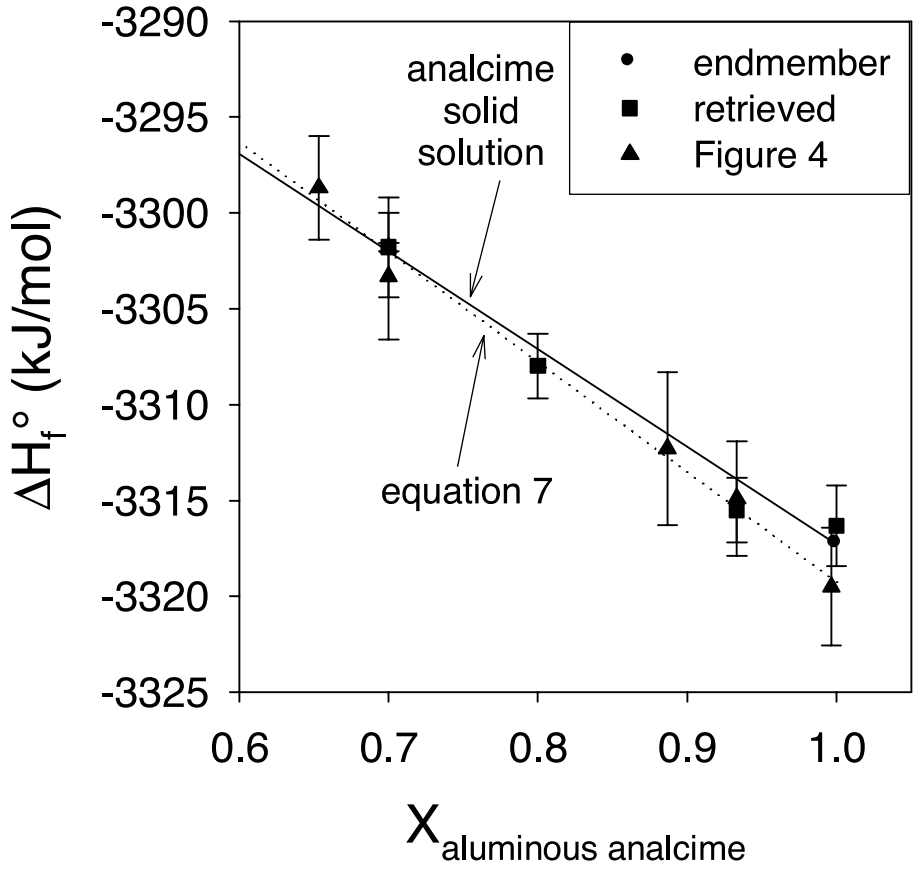

Fig. 12. Enthalpies of formation at 25°C from figure 4 (triangles) for low analcime and those retrieved in this study for endmember aluminous analcime (circle) and for samples from the experiments summarized in figures 8–11 (squares) as a function of the mol fraction of the aluminous endmember. The dotted line refers to the least squares linear regression in equation (7) and the solid line is the mixing trend between siliceous and aluminous endmember low analcime generated in this study.

(24; calculated in this study) and the activities of aluminous and siliceous low analcime in the respective samples. It can be seen in figures 10 and 11 that there is generally excellent agreement between the calculated solubility of analcime and that measured experimentally.

The retrieved enthalpies of formation at 298.15 K, 1 bar listed in table 7 are plotted in figure 12 as a function of $X_{aluminous}$. In figure 12, ΔH_f° retrieved from the studies summarized above are plotted for the respective compositions of analcimes used in the experiments (squares) along with ΔH_f° for the aluminous low analcime (circle) and the values of ΔH_f° derived from calorimetric data for the more stable trend in figure 4 (triangles). Shown for comparison are a linear trend of ΔH_f° between ΔH_f° for the aluminous and siliceous low analcime endmembers (solid line) corresponding to the variation of ΔH_f along the solid solution, and the least squares regression of the calorimetric data (eq 7; dotted line). It can be seen that there is excellent agreement between the retrieved and calorimetrically-derived values of ΔH_f°, and that both data sets are consistent with the solid solution model retrieved from experimental equilibrium observations. The difference between the trend implied by equation (7) and the

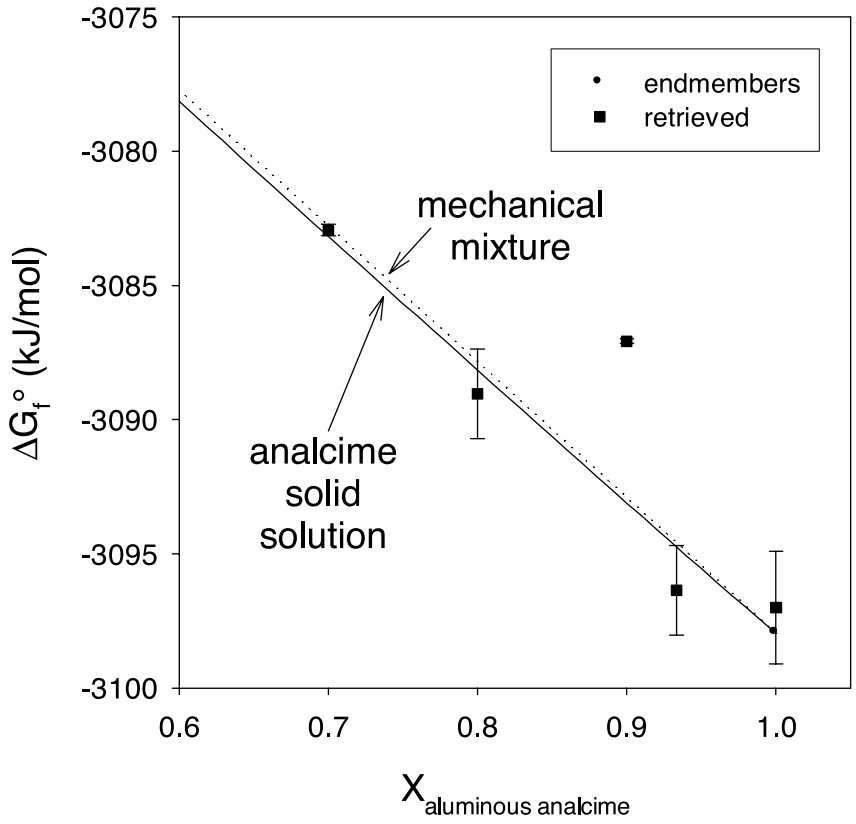

Fig. 13. Gibbs energies of formation at 25°C retrieved in this study for endmember aluminous analcime (circle) and for samples from the experiments summarized in figures 8–11 (squares) as well as that of Murphy and others (1996; outlying point) as a function of the mol fraction of the aluminous endmember. The dotted line represents the mechanical mixing trend between siliceous and aluminous endmember low analcime generated in this study and the solid curve corresponds to the solid solution model derived in this study.

mixing trend between aluminous and siliceous low analcime is well within the uncertainties of the coefficients in equation (7). This similarity is evidenced by the reasonable agreement between ΔH_f° retrieved for siliceous low analcime (−3266.4 kJ/mol) and that calculated from equation (7); (−3261.9 kJ/mol).

Figure 13 depicts the values of ΔG_f° retrieved in the present study for the respective compositions of analcimes used in the experiments (squares) along with ΔH_f° for aluminous low analcime (circle). Shown for comparison is the trend in ΔG_f° consistent with the solid solution model and thermodynamic properties derived above (solid line) and the mechanical mixing trend between aluminous and siliceous low analcime (dotted line). Although the solid solution is stable with respect to a mechanical mixture at all compositions shown on the plot (a relationship that holds over the whole range of the solid solution), the energetic separation between the solid solution and a mechanical mixture is relatively small. This relationship is consistent with previous observations of analcime solid solutions (Wise, 1984; Wilkin and Barnes, 1998). The observations suggested that ΔG_f° varies linearly with composition in analcime. Contrary to the suggestion of Wise (1984), however, this does not imply that analcime solid solutions are ideal. The distinct non-ideality of analcime solid solutions is evidenced by

the difference between the activity-composition relationships for an ideal solid solution and the athermal solution observed in low analcime that are depicted in figure 7. It can be seen that, with the exception of the datum from Murphy and others (1996), all of the retrieved values of ΔG_f° for the experimental analcime compositions are consistent with the solid solution model derived in this study. The datum from Murphy and others (1996) was calculated from tightly reversed observations of the solubility of analcime (reaction 24) at 298.15 K, 1 bar. Careful consideration of the experimental techniques and results of Murphy and others (1996) reveals no reason to suspect that this datum is erroneous. This conclusion suggests that the Murphy and others' (1996) sample is significantly less stable for its composition (~6 kJ/mol) than the other samples considered in the retrieval calculations.

ENERGETICS OF SI-AL DISORDER IN ANALCIME

The ^{29}Si MAS NMR, calorimetric, and phase equilibrium data discussed above clearly indicate the presence of at least two distinct states of Si-Al ordering in analcime. In addition to high and low analcime, which exhibit different modes of short range ordering (Al avoidance and Al-O-Si-O-Al avoidance, respectively), the study of Kohn and others (1995) suggests the existence of long range Si-Al ordered analcime. The data presented above do not indicate the presence of transitional states between long range ordered, low, and high analcime. Consequently, in the discussion below, it is assumed that the transitions between these phases are discrete first order transitions. Based on the geologic and thermodynamic arguments below, it appears that these distinct ordering states are reflective of temperature of formation. Indeed, Second Law considerations indicate that long range ordered analcime should be stable at the lowest temperatures, and high analcime stable at the highest temperatures.

The apparent rarity of long range ordered analcime is likely a consequence of a very low temperature of transition between long range ordered analcime and low analcime. Unfortunately, there does not appear to be any experimental data pertinent to evaluating the thermodynamic properties of this transition. However, Dove and others (1996) describe statistical mechanical calculations concerning the temperature of transition of long range ordered to short range ordered leucite, which share the ANA framework with analcime. Short range ordered leucite exhibits the framework Si-Al distribution of high analcime (Phillips and Kirkpatrick, 1994). Using an adjusted Bragg-Williams model, Dove and others (1996) predicted a very low temperature of disordering, on the order of 310 K. If these calculations are correct, then the rarity of long range ordered analcime might be due to the fact that most analcime formation occurs at temperatures above the transition temperature. It is possible that low analcime forms in very low temperature parageneses in a metastable state of Si-Al disorder.

The results of the present study bear directly on the next order-disorder transition in analcime, that from low analcime to high analcime. The Gibbs energy ($\Delta G_{dis,298.15}$), enthalpy ($\Delta H_{dis,298.15}$) and entropy ($\Delta S_{dis,298.15}$) of the disordering transition between low and high analcime at 298.15 K, 1 bar are related through:

$$\Delta G_{dis,298.15} = \Delta H_{dis,298.15} - 298.15\Delta S_{dis,298.15}. \quad (33)$$

The properties of disordering in equation (33) are dependent on the composition of analcime, and in the discussion below we consider only the properties of this transition for the composition of ANA-MSHO (high analcime) and ANA-MSHG (low analcime). The difference between the calorimetric observations of ΔH_{sol} for ANA-MSHO and ANA-MSHG (6.1 ± 3.0 kJ/mol) is equal to $\Delta H_{dis,298.15}$ (although the measurements were conducted at 323 K, the heat content differences over this 25 K interval are certainly much smaller than the standard error in ΔH_{sol}) . Assuming a negligible

difference in $S_{0\rightarrow 298.15}$ between high and low analcime (as noted in the feldspars; Openshaw and others, 1976), $\Delta S_{dis,298.15}$ is represented by the difference between the low and high analcime trends in figure 2. As noted above, the analcime sample studied by Murphy and others (1996) appears to be energetically distinct from the low analcime solid solution considered above. Their sample came from Mont St. Hilaire (Canada), the same locality as ANA-MSHO, ANA-MSHG, and the analcime studied by Wilkin and Barnes (1998). The composition of Murphy and others' (1996) sample is essentially identical to that of ANA-MSHO and ANA-MSHG, which facilitates direct comparison of their thermodynamic properties, and its instability relative to the low analcime solid solution described above is consistent with it being high analcime. The difference in ΔG_f between the sample of Murphy and others (1996) and the solid solution described above (6 ± 0.1 kJ/mol) is taken here to be a measure of $\Delta G_{dis,298.15}$. The fact that $\Delta G_{dis,298.15}$ calculated from the Murphy and others' (1996) sample is similar in magnitude to $\Delta H_{dis,298.15}$ determined calorimetrically supports this interpretation. For instance, if one assumes that $\Delta S_{dis,298.15} = 3.5$ J/molK and $\Delta G_{dis,298.15} = 6$ kJ/mol, then $\Delta H_{dis,298.15} = 7.0$ kJ/mol is consistent with the calorimetric results obtained in this study.

If one assumes that the heat capacity of disordering is negligible (which is consistent with the behavior of alkali feldspars; Helgeson and others, 1978), then equation (33) can be used to predict the temperature of disordering (T_{dis}) at 1 bar pressure by noting that at the transition temperature, $\Delta G_{dis,298.15} = 0$ and thus

$$T_{dis} = \Delta H_{dis,298.15} / \Delta S_{dis,298.15}. \quad (34)$$

Taking $\Delta H_{dis,298.15} = 7$kJ/mol and $\Delta S_{dis,298.15} = 3.5$ J/molK, the temperature of transition thus calculated is 2000 K, although the calorimetric observations of $\Delta H_{dis,298.15}$ are permissive of a transition temperature as low as ~885 K. These temperatures are higher than presumed for analcime formation in most environments, and may be higher than the actual transition temperature. For instance, based on samples ANA-MSHG and ANA-MSHO, it appears that low and high analcimes coexist in hydrothermal systems around alkaline intrusive complexes such as Mont St. Hilaire. Markl (2001) estimated the temperatures of formation for analcime-bearing assemblages in the Ilimaussaq alkaline intrusive complex at ~300°–460°C (570-730 K). In addition, Kim and Burley (1980) observed a phase transition in analcime based on relatively small variations in unit cell dimensions obtained for experimental run products formed at temperatures between 350° and 400°C at 2 kbar. This transition was quenched, suggesting that it is not a displacive transition such as those observed in other tectosilicates. Although the degree of Si-Al disorder accompanying their samples is unknown, the temperature of this transition is coincident with the inferred temperature of analcime parageneses in alkaline intrusions. Due to the very small volume change accompanying the transition observed by these authors, the temperature of this transition is likely not a sensitive function of pressure (although the Clapeyron slope for the transition would be negative as the low temperature phase had a larger molar volume). If the phase transition observed by Kim and Burley (1980) were the disordering transition proposed in this study (and apparently observed in analcime parageneses in alkaline intrusive complexes), then there would appear to be a significant discordance between the thermodynamic data generated in this study and the disordering behavior of analcime.

While the apparent instability of high analcime at conditions present in Earth's crust based on the thermodynamic properties generated in this study may reflect errors in derivation of these properties, this may not be the cause of this discrepancy. An alternative explanation for this discrepancy may lie in the dehydration behavior of analcime. The thermodynamic properties of disordering between low and high

analcime discussed above pertain to the fully hydrated state. It is possible that the transition occurs under conditions where either low analcime or high analcime (or both) is (are) fully or partially dehydrated. A relatively small difference in the enthalpy of dehydration of low and high analcime (on the order of 4 kJ/mol of analcime) would be sufficient to bring T_{dis} calculated from equation (34) for dehydrated analcime into the temperature range suggested by the observations noted above. The topologies of thermogravimetric curves for hydrothermal analcimes and analcimes replacing leucites in ultrapotassic volcanic rocks (which are similar in habit to ANA-MSHO, and likely inherited the high analcime Si-Al distribution form leucite) suggest that the enthalpy of dehydration is different between these two populations (Giampaolo and Lombardi, 1994). Leucite-derived analcimes, which may form via ion exchange at relatively high temperatures, exhibit weight loss curves that are much more gradual than hydrothermal analcimes, suggesting that the enthalpy of dehydration is less positive for leucite-derived analcimes than for hydrothermal analcimes (see Bish and Carey, 2001). This observation appears to be consistent with the energetic effect necessary to stabilize dehydrated high analcime to lower temperatures than the hydrated phase. Whereas data are not available to rigorously test this hypothesis, experiments are planned to determine the differences in the enthalpies of dehydration in low and high analcime.

geologic phase relations involving low analcime

A further test of the validity of the solid solution model derived above and the thermodynamic data presented in tables 6 and 7 is provided by comparison of compositional and phase relations involving low analcime with observations from natural systems. Analcime is one of the most common rock-forming zeolites at shallow levels in the earth's crust, and exhibits a large compositional range in these environments. Natural parageneses in diagenetic and low grade metamorphic systems indicate that the stability field of low analcime is bounded by the stability of other zeolites (for instance, natrolite, clinoptilolite, phillipsite, and mordenite) and albite (Hay, 1966; Iijima, 1978, 1988). Thermodynamic data for other Na-rich zeolites are presently inadequate to rigorously describe equilibria with low analcime. However, chemical and thermobarometric isograds between low analcime and albite have been described in numerous locations, and provide a means of assessing the prograde stability of low analcime during regional metamorphism. The controls on low analcime composition in the earth's crust and its stability with respect to albite are discussed below with the aid of phase diagrams calculated from the thermodynamic properties summarized in tables 6 and 7.

As noted above, the presence of a $SiO_2 \cdot 0.5\ H_2O$ exchange vector in low analcime solid solutions indicates that (for a given chemical potential of H_2O) analcime composition is controlled by the chemical potential of SiO_2. This control can be described by reaction (28), which describes equilibrium between low analcime and $SiO_{2(aq)}$ in coexisting aqueous solutions. It can be seen from the mass action expression for reaction (28; eq 29) that at constant temperature, pressure, and chemical potential of H_2O, the composition of analcime can be described solely in terms of $a_{SiO_2(aq)}$. This relationship is exploited in figure 14, which depicts isopleths of constant analcime composition as a function of temperature and log $a_{SiO_2(aq)}$ at pressures corresponding to the liquid-vapor saturation curve for pure H_2O (P_{SAT}). Shown for comparison are the compositions of solutions in equilibrium with quartz, chalcedony, and amorphous silica at these conditions.

It can be seen in figure 14 that the composition of low analcime at temperatures near the earth's surface can vary widely depending on log $a_{SiO_2(aq)}$. Compositions approaching the aluminous endmember are stable only in quartz undersaturated conditions (which holds over the whole range of conditions in figure 14). This

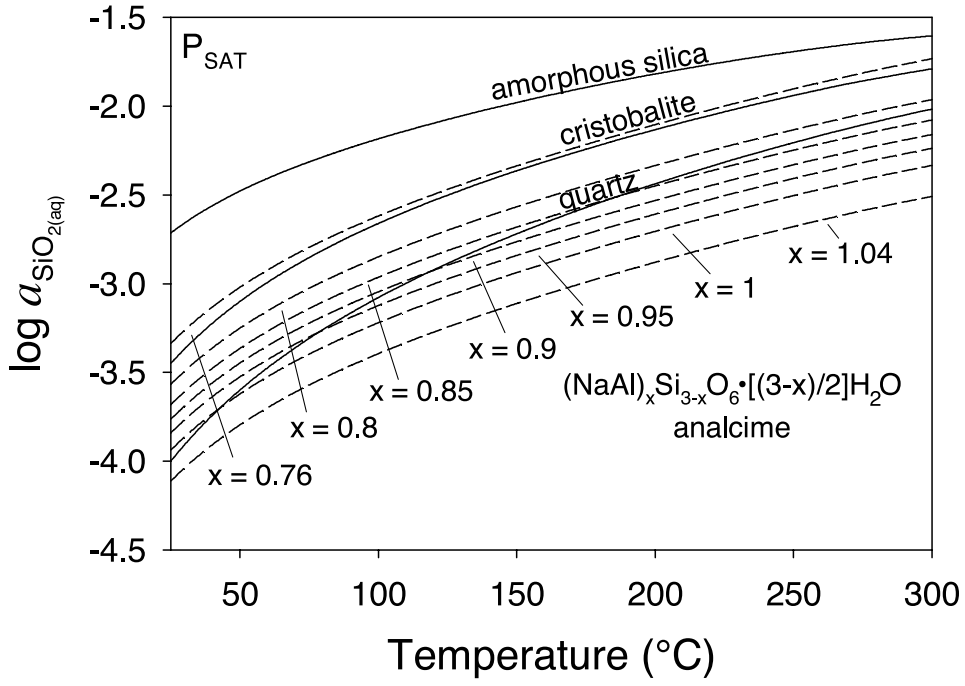

Fig. 14. Isopleths of constant analcime composition (dashed curves) as a function of aqueous silica activity and temperature at pressures corresponding to liquid-vapor equilibrium for water. Shown for comparison are the activities of aqueous silica in equilibrium with quartz, chalcedony, and amorphous silica.

composition-dependence is consistent with the observation that the low temperature parageneses in which low analcime coexists with the silica-poor zeolite natrolite (Wise, 1984) never occurs with quartz. This parageneses typically occurs in silica-poor environments such as that where ANA-SBC formed. In contrast, the most Si-rich low analcimes known, whose compositions approach that of the siliceous endmember (Broxton and others, 1987), typically coexists with cristobalite or other metastable silica polymorphs. Inspection of figure 14 suggests that the composition of low analcime in metastable equilibrium with cristobalite is essentially invariant with respect to temperature. In contrast, the relations shown in figure 14 suggest that the composition of low analcime in equilibrium with quartz is sensitive to temperature, with Si content increasing markedly as temperature increases. This contrast in behavior is a direct consequence of the fact that $\Delta\bar{H}_f$ $SiO_2 \cdot 0.5H_2O$ is similar to ΔH_f° of (cristobalite + 0.5 H_2O), which has a value that is less stable than ΔH_f° of (quartz + 0.5 H_2O).

The topology of figure 14 is sensitive to the choice of thermodynamic properties of aqueous silica used in the calculations. Recently, Rimstidt (1997) and Gunnarsson and Arnórsson (2000) used new experimental determinations of quartz and amorphous silica solubility, respectively, to suggest that at low temperatures (below ~150 °C) the solubility of the silica polymorphs is greater than indicated in figure 14. For instance, at 25°C, 1 bar, Rimstidt (1997) determined the solubility of quartz to be ~11 ppm, as opposed to ~6 ppm as indicated by Walther and Helgeson (1977; the source of the curve in fig. 14), Fournier and Potter (1982) and Manning (1994). If the observations of Rimstidt (1997) and Gunnarsson and Arnórsson (2000) were correct, then aqueous silica would have to be more stable at lower temperatures. Such a stabilization of aqueous silica would lead to slight changes in the topology of figure 14,

namely a decrease in the slopes of the curves at low temperatures and a displacement of all of the curves to slightly higher values of log $a_{SiO_2(aq)}$. However, because these effects are nearly equal for the analcime composition isopleths and the silica polymorph solubilities in figure 14, the qualitative aspects of phase relations between these minerals discussed above would not appreciably be affected if one were to adopt more stable values for the thermodynamic properties of $SiO_{2(aq)}$.

Saha (1961) suggested that low analcime compositions coexisting with quartz could be used as a geothermometer; however, both he and Coombs and Whetten (1967) suggested that low analcime in equilibrium with quartz should become more aluminous with increasing temperature, as H_2O appears with the aluminous endmember in reaction (28), suggesting that the entropy change across the reaction

$$0.75(NaAl)_{1.05}Si_{1.95}O_6 \cdot 0.975H_2O + 0.9SiO_{2(quartz)} + 0.45H_2O = 1.05(NaAl)_{0.75}Si_{2.25}O_6 \cdot 1.125H_2O \quad (35)$$

should be negative. However, the partial molar entropy of $SiO_2 \cdot 0.5H_2O$ consistent with the data in table 7 is larger than S° of (quartz + 0.5 H_2O), which agrees with the observation that S° for pure silica zeolites is generally larger than that of quartz (Boerio-Goates and others, 2002). As noted by Coombs and Whetten (1967), there is little indication in the geologic record for systematic changes in the composition of low analcime coexisting with quartz as a function of temperature within burial metamorphic systems. One explanation for this observation is that low analcime compositions commonly reflect the composition of materials from which they formed (Coombs and Whetten, 1967; Ogihara, 1996) and they typically form at relatively low temperatures under quartz-supersaturated conditions. These relationships lead to low temperature analcimes typically having relatively silicic composition because as temperature increases and quartz enters the assemblage, there is little thermodynamic drive for re-equilibration. Metastable persistence of analcimes with compositions out of equilibrium with quartz is probably the rule rather than the exception. This persistence may in large part be a consequence of the relatively small stabilization energy of low analcime solid solutions noted above.

Figure 15 shows isopleths of constant low analcime composition in stable and metastable equilibrium with quartz and water calculated from the thermodynamic properties of reaction (35) (dashed curves; low analcime compositions indicated by labels superimposed on the curves) as a function of temperature and pressure. Also shown are isopleths of low analcime composition in metastable equilibrium with albite, quartz and water (dotted curves) calculated from the properties of the reaction

$$1.05\underset{\text{albite}}{NaAlSi_3O_8} + 0.975H_2O = (NaAl)_{1.05}Si_{1.95}O_6 \cdot 0.975H_2O + 1.2SiO_{2(quartz)} \quad (36)$$

It can be seen that both increasing temperature and pressure favor an increase in the Si content of low analcime with respect to reactions (35) and (36). The intersections of isopleths of equilibrium low analcime composition with respect to reactions (35) and (36) defines the stable univariant curve (solid curve in fig. 15) separating the stability field of low analcime + quartz at relatively low temperatures and pressures from that of albite + water at relatively high temperatures and pressures. Inspection of figure 15 shows that the Si content of low analcime along the stable univariant curve for reaction (36) increases with increasing temperature/decreasing pressure.

Reaction (36) has been the subject of several phase equilibrium investigations (Campbell and Fyfe, 1965; Thompson, 1971; Liou, 1971), the results of which at $P < 4$ kbar are summarized by the symbols in figure 15. The arrows above the symbols

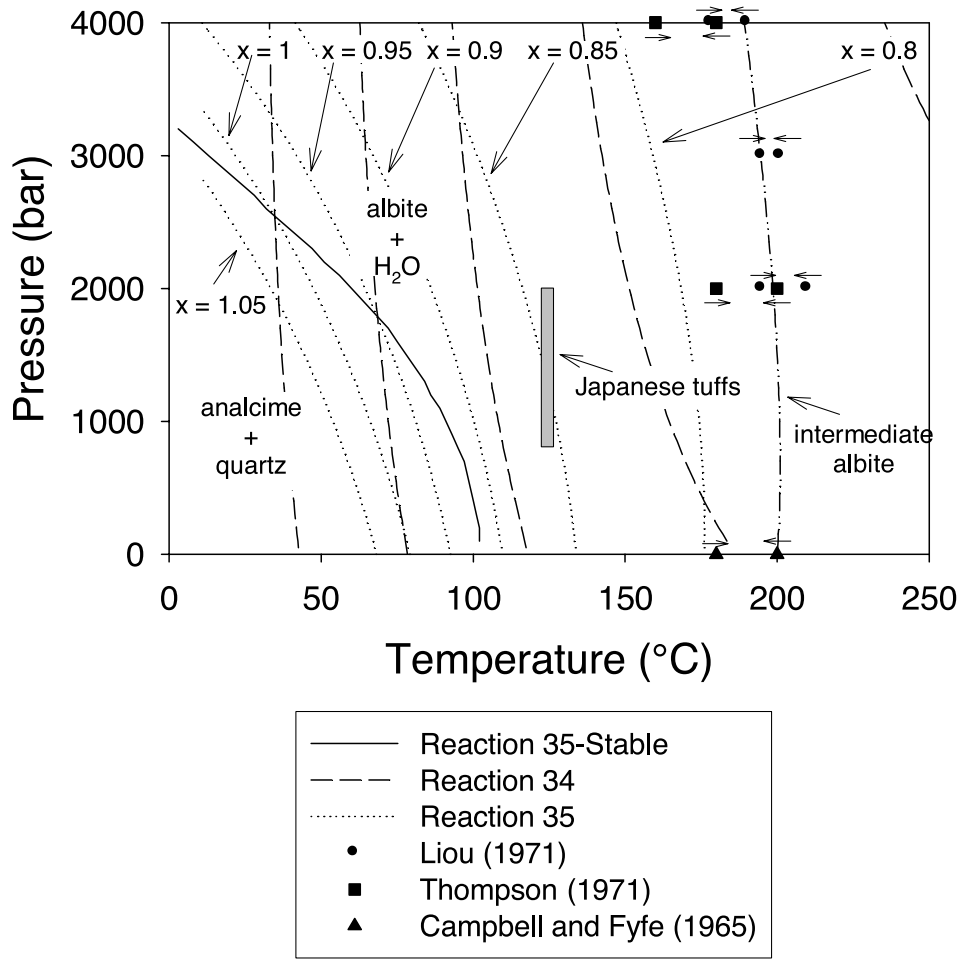

Fig. 15. Isopleths of constant analcime composition in equilibrium with quartz and water (dashed curves; compositional labels are superimposed on curves) and albite, quartz, and water (dotted curves) as a function of temperature and pressure. Also shown is the stable univariant curve for the prograde breakdown of analcime + quartz to albite + water (solid curve). The symbols are experimental observations of equilibrium between analcime, albite, quartz, and water; the dash-dot-dot curve is discussed in the text and corresponds to equilibrium between the analcime used by Liou (1971) and a metastable, partially disordered albite. The gray box labeled "Japanese tuffs" represents the thermobarometric conditions observed by Iijima (1978, 1988) for equilibrium between analcime, albite, quartz, and water in diagenetically altered tuffs deposited in geosynclinal basins in Japan.

indicate the direction of reaction progress at each point in temperature-pressure space; arrows pointing to the right indicate formation of low analcime + quartz at the expense of albite, arrows pointing to the left indicate formation of albite at the expense of low analcime + quartz. It can be seen that there is a substantial disparity between the stable curve for reaction (36) and the experimental phase equilibrium observations, with the latter suggesting that reaction (36) occurs at significantly higher temperatures than calculated in this study.

This discrepancy can readily be explained by consideration of the experimental techniques and starting materials used in the respective studies depicted in figure 15. The analcime used as a starting material in Liou's (1971) and Thompson's (1971)

experiments had a composition of $(NaAl)_{0.96}Si_{2.04} \cdot 1.02H_2O$; Campbell and Fyfe (1965) did not report the composition of the starting materials in their experiments. In any event, in all cases, if analcime composition did not vary with temperature, then the phase equilibrium observations would apparently pertain to metastable equilibrium between the starting analcime and albite, quartz, and H_2O. Thompson (1971) and Campbell and Fyfe (1965) inferred forward and reverse progress for reaction (36) at a given temperature and pressure by monitoring the change in mass of a single crystal of one (or two) of the solid phases participating in the reaction. This method is subject to considerable complications, including irreversible dissolution of the single crystal and uncertainties in the identity, crystallinity, and ordering state of phases precipitated during the experiments. The mass of albite was monitored in all experiments reported by Thompson (1971) and Campbell and Fyfe (1965). Monitoring of the mass of a high temperature phase (in this case, albite) that undergoes irreversible dissolution would elevate the inferred equilibrium temperature (Kerrick, 1968; Thompson, 1970). In addition, Thompson (1971) and Campbell and Fyfe (1965) did not monitor the ordering state of albite in their studies. The generally good agreement between their results and those of Liou (1971) suggests that metastable disorder in albite may explain the differences between the curve generated in this study and the results of hydrothermal weight loss experiments.

Liou (1971) investigated reaction (36) through traditional phase equilibrium techniques and was able to demonstrate reversible equilibrium by monitoring changes in X-ray diffraction peaks of the experimental charges. However, Liou's (1971) experiments pertain to equilibrium between analcime, quartz, and a *metastable* disordered albite, rather than the low albite used by Campbell and Fyfe (1965) and Thompson (1971). Furthermore, it is clear from the XRPD peak spacing data reported by Liou (1971) that while analcime likely did not change composition during his experiments, the ordering state of the albite did. Unfortunately Liou (1971) did not report unit cell edges for the albite in his experiments, precluding estimation of the degree of Si-Al order. Trial and error calculations using the thermodynamic properties for analcime, generated in this study and those of low and high albite, from Helgeson and others (1978), indicates that Liou's (1971) results pertain to equilibrium between his starting analcime and albite that has a Z ordering parameter (Thompson and others, 1974) of ~0.67. This value requires that the albite was more ordered than suggested by the conditions under which the starting albite was synthesized. This result is consistent with partial ordering of albite during the course of the experiments. The metastable univariant curve generated in these calculations is shown by the dash-dot-dot curve labeled "intermediate albite" in figure 15. The large displacement of the univariant curve for reaction (36) due to disordering in albite is a consequence of the small entropy of reaction, which is generally less than 25 J/mol of reaction at the conditions represented in figure 15. These considerations, and the geologic observations summarized in the next paragraph, indicate that direct application of the experimental studies of Campbell and Fyfe (1965), Thompson (1971) and Liou (1971) to the thermobarometric conditions attending equilibrium between analcime, albite, quartz and H_2O in geologic systems leads to significant overestimates of thermal conditions within the crust and associated inferences about thermal gradients and heat flow.

Geologic observations of the temperature-pressure conditions attending equilibrium with respect to reaction (36) are limited but in excellent agreement with the relations presented in figure 15. The one observation of which we are aware for the conversion of low analcime to albite at quartz saturation in a natural system undergoing active alteration is that of Iijima (1978, 1988) from geosynclinal silicic tuffs in Japan (box labeled "Japanese tuffs" in fig. 15). Reaction (36) is apparently in equilibrium

over broad areas in Japan at temperatures of ~120° −124 °C and pressure of 1–2 kbar. Low analcime in these systems forms initially from clinoptilolite precursors (Ogihara, 1996) and throughout the system has a relatively uniform composition with respect to depth (temperature and pressure) of ~ $(NaAl)_{0.85}Si_{2.15}O_6 \cdot 1.075H_2O$ (Iijima, 1978). The conditions where this analcime is observed transforming in the presence of quartz to albite overlaps the metastable curve generated in this study for equilibrium with respect to reaction (36) for an analcime of this composition. It thus appears that analcime is stabilized in these occurrences by its relatively high Si content, and the conditions of its prograde transformation to albite in the presence of quartz are consistent metastable equilibrium with respect to reaction (36) for its composition. Observations from fossil systems also seem to be consistent with this conclusion and with the temperature dependence of the composition of analcime in metastable equilibrium with respect to reaction (36). An apparent isograd between amygdaloidal analcime (with $n_{Al} = 2$ to 2.05) and albitized plagioclase in the presence of chalcedony (that is, slightly higher chemical potential of SiO_2 than associated with the presence of quartz) occurs in metabasites in Iceland at crustal depths associated with a temperatures of 70° to 80 °C and pressures of 200 to 300 bars (Fridriksson and others, 2001; Neuhoff, unpublished data). It can be seen in figure 15 that the thermobarometric conditions associated with this isograd are in excellent agreement with the relevant isopleths of low analcime composition in metastable equilibrium with reaction (36). Iijima and Hay (1968) reported the occurrence of analcime with $n_{Al} > 1$ in saline lake sediments of the Green River Formation in Wyoming (USA) associated with authigenic quartz and authigenic K-feldspar and albite. If this assemblage formed at Earth surface conditions, it can be inferred from figure 15 that equilibrium between low analcime, albite and quartz is not possible in this system. This result is consistent with Iijima and Hay's (1968) observations that quartz and feldspar content in the system are inversely related. Nonetheless, the fact that low analcime of such low Si content formed under these conditions in equilibrium with quartz and near equilibrium with albite is consistent with the general trends apparent in figures 14 and 15. It appears from these relationships that predictions of low analcime stability and composition in geologic systems generated using the thermodynamic properties summarized in tables 6 and 7 are reasonable.

CONCLUDING REMARKS

Spectroscopic, calorimetric, and compositional data, combined with theoretical considerations of the energetic consequences of solid solution in low analcime and experimental equilibrium observations, were used in this study to derive thermodynamic properties for low analcime solid solutions that are in excellent agreement with not only the experimental observations, but also geologic observations of analcime stability and composition. Additional observations support the presence of at least two distinct states of Si-Al disorder in natural and synthetic analcimes. It is clear that further investigation of the energetics of high analcimes, along with experimental equilibrium observations and determination of the energetics of dehydration in low and high analcimes, are necessary in order to predict the conditions associated with a potential order-disorder transition in this material and to evaluate the stability of analcime in high temperature geologic environments. This investigation is particularly relevant to understanding the stability of analcime with respect to isostructural phases such as leucite, pollucite, and wairakite. Whereas Na^+ is the dominant extraframework cation in low analcimes, analcimes formed at relatively high temperatures in geologic and experimental systems can display considerable solution of Ca^{+2} (as in wairakite; Seki and Oki, 1969), Cs^+ (as in pollucite; Teertstra and others, 1994), and other ions in the interchannel sites. It appears that attempts to assess the properties of solid

solutions between analcime and isostructural materials such as wairakite, pollucite, and Rb-analcime should consider high analcime as the Na-endmember.

ACKNOWLEDGMENTS

This study was supported by the U.S. National Science Foundation (grants EAR-0104926 to JFS and EAR-00000523 to GLH) and the University of Florida. J. Apps is thanked for providing data from his unpublished thesis and for discussions and unpublished calculations concerning silica solubility. S. Kleine generously donated samples for this study. Th. Fridriksson provided a helpful review of an earlier version of the manuscript. The manuscript benefited from helpful discussions with C. Manning and insightful reviews by J. Roux, J. Apps, B. Phillips, and J.W. Carey.

References

Apps, J. A., ms, 1970, The stability field of analcime: Ph.D. thesis, Harvard University, Cambridge, 347 p.

Barany, R., 1962, Heats and free energies of formation of some hydrated and anhydrous sodium- and calcium-aluminum silicates: United States Bureau of Mines Report of Investigations 5900, 17 p.

Benson, S. W., 1968, Thermochemical kinetics: New York, John Wiley and Sons, 223 p.

Bish, D. L., and Carey, J. W., 2001, Thermal properties of natural zeolites, *in* Bish, D. L., and Ming, D. W., editors, Natural Zeolites: Occurrence, Properties, Applications: Mineralogical Society of America and the Geochemical Society Reviews in Mineralogy and Geochemistry, v. 45, p. 403–452.

Boerio-Goates, J., Stevens, R., Hom, B. K., Woodfield, B. F., Piccione, P. M., Davis, M. E., and Navrotsky, A., 2002, Heat capacities, third-law entropies and thermodynamic functions of SiO_2 molecular sieves from $T = 0$ K to 400 K: Journal of Chemical Thermodynamics, v. 34, p. 205–227.

Broxton, D. E., Bish, D. L., and Warren, R. G., 1987, Distribution and chemistry of fracture-lining zeolites at Yucca Mountain, Nye County, Nevada: Clays and Clay Minerals, v. 35, p. 89–110.

Campbell, A. S., and Fyfe, W. S., 1965, Analcime-albite equilibria: American Journal of Science, v. 263, p. 807–816.

Coombs, D. S., and Whetten, J. T., 1967, Composition of analcime from sedimentary and burial metamorphic rocks: Geological Society of America Bulletin, v. 78, p. 269–282.

Cruciani, G., and Gualtieri, A., 1999, Dehydration dynamics of analcime by in situ synchrotron powder diffraction: American Mineralogist, v. 84, p. 112–119.

Dove, M. T., Thayaparam, S., Heine, V., and Hammonds, K. D., 1996, The phenomenon of low Al-Si ordering temperatures in aluminosilicate framework structures: American Mineralogist, v. 81, p. 349–362.

Engelhardt, G., and Michel, D., 1987, High-resolution solid-state NMR of silicates and zeolites: New York, John Wiley and Sons, 485 p.

Fournier, R. O., and Potter, R. W., 1982, An equation correlating the solubility of quartz in water from 25°C to 900°C at pressures up to 10,000 bars: Geochimica et Cosmochimica Acta, v. 46, p. 1969–1973.

Fridriksson, Th., Neuhoff, P. S., Arnórsson, S., and Bird, D. K., 2001, Geological constraints on the thermodynamic properties of the stilbite-stellerite solid solution in low-grade metabasalts: Geochimica et Cosmochimica Acta, v. 65, p. 3993–4008.

Giampaolo, C., and Lombardi, G., 1994, Thermal behavior of analcimes from two different genetic environments: European Journal of Mineralogy, v. 6, p. 285–289.

Gunnarsson, I., and Arnórsson, S., 2000, Amorphous silica solubility and the thermodynamic properties of $H_4SiO_4^\circ$ in the range of 0° to 350°C at P_{sat}: Geochimica et Cosmochimica Acta, v. 64, p. 2295–2307.

Hay, R. L., 1966, Zeolites and Zeolitic Reactions in Sedimentary Rocks: Geological Society of America Special Paper 85, 130 p.

He, H. Y., Cheng, C. F., Seal, S., Barr, T. L., and Klinowski, J., 1995, Solid-state NMR and ESCA studies of the framework aluminosilicate analcime and its gallosilicate analog: Journal of Physical Chemistry, v. 99, p. 3235–3239.

Helgeson, H. C., Delany, J. M., Nesbitt, H. W., and Bird, D. K., 1978, Summary and critique of the thermodynamic properties of rock-forming minerals: American Journal of Science, v. 278-A, 229 p.

Herreros, B., and Klinowski, J., 1995, Hydrothermal synthesis of zeolites from 5-coordinate silicon compounds: Journal of Physical Chemistry, v. 99, p. 1025–1029.

Holland, T. J. B., and Redfern, S. A. T., 1997, Unit-cell refinement: Changing the dependent variable, and use of regression diagnostics: Mineralogical Magazine, v. 61, p. 65–77.

Hovis, G. L., 1982, Resolution of a systematic interlaboratory discrepancy in recent calorimetric data, and the heats of solution of quartz, low albite, adularia, and gibbsite: American Mineralogist, v. 67, p. 950–955.

——— 1988, Enthalpies and volumes related to K-Na mixing and Al-Si order/disorder in alkali feldspars: Journal of Petrology, v. 29, p. 731–763.

Hovis, G. L., and Roux J., 1993, Thermodynamic mixing properties of nepheline - kalsilite crystalline solutions: American Journal of Science, v. 293, p. 1108–1127.

Hovis, G. L., Roux, J., and Richet, P., 1998, A new era in hydrofluoric acid solution calorimetry: Reduction of required sample size below ten milligrams: American Mineralogist, v. 83, p. 931–934.

Hovis, G. L., Roux, J., and Rodrigues, E., 2002, Thermodynamic and structural behavior of analcime-leucite analogue systems: American Mineralogist, v. 87, p. 523–532.

Iijima, A., 1978, Geological occurrences of zeolite in marine environments, *in* Sand, L. B., and Mumpton, F. A., editors, Natural Zeolites: Occurrence, Properties, and Applications: New York, Pergamon Press, p. 175–198.

——— 1988, Diagenetic transformations of minerals as exemplified by zeolites and silica minerals; a Japanese view, *in* Chilingarian, G. V., editor, Diagenesis II, Developments in Sedimentology 43: Amsterdam, Elsevier, p. 147–209.

Iijima, A., and Hay, R. L., 1968, Analcime composition in tuffs of the Green River Formation of Wyoming: American Mineralogist, v. 53, p. 184–200.

Johnson, G. K., Flotow, H. E., O'Hare, P. A. G., and Wise, W. S., 1982, Thermodynamic studies of zeolites: Analcime and dehydrated analcime: American Mineralogist, v. 67, p. 736–748.

Johnson, J. W., Oelkers, E. H., and Helgeson, H. C., 1992, SUPCRT92: Software package for calculating the standard molal thermodynamic properties of minerals, gases, aqueous species, and reactions among them as functions of temperature and pressure: Computers in Geoscience, v. 18, p. 899–947.

Joshi, P. N., Thangaraj, A., and Shiralkar, V. P., 1991, Studies on zeolite transformation of high-silica gmelinite into analcime: Zeolites, v. 11, p. 164–168.

Kato, M., and Hattori, T., 1998, Ordered distribution of aluminum atoms in analcime: Physics and Chemistry of Minerals, v. 25, p. 556–565.

Kerrick, D. M., 1968, Experiments on the upper stability of pyrophyllite at 1.8 kb and 3.9 kb water pressure: American Journal of Science, v. 266, p. 204–214.

Kikuchi, R., 1951, A theory of cooperative phenomena: Physical Review, v. 81, p. 988–1003.

Kim, K. T., and Burley, B. J., 1980, A further study of analcime solid solutions in the system $NaAlSi_3O_8$ -$NaAlSiO_4$ -H_2O, with particular note of an analcime phase transformation: Mineralogical Magazine, v. 43, p. 1035–1045.

Klinowski, J., Ramdas, S., Thomas, J. M., Fyfe, C. A., and Hartman, J. S., 1982, A re-examination of Si, Al ordering in zeolites NaX and NaY: Journal of the Chemical Society-Faraday Transactions II, v. 78, p. 1025–1050.

Kohn, S. C., Henderson, C. M. B., and Dupree, R., 1995, Si-Al order in leucite revisited - New information from an analcite-derived analog: American Mineralogist, v. 80, p. 705–714.

Kubaschewski, O., Alcock, C. B., and Spencer, P. J., 1993, Materials Thermochemistry: Oxford, Pergamon, 363 p.

Liou, J. G., 1971, Analcime equilibria: Lithos, v. 4, p. 389–402.

Lippmaa, E., Magi, M., Samoson, A., Tarmak, M., and Engelhardt, G., 1981, Investigation of the structure of zeolites by solid-state high-resolution ^{29}Si NMR Spectroscopy: Journal of the American Chemical Society, v. 103, p. 4992–4996.

Loewenstein, W., 1954, The distribution of aluminum in the tetrahedra of silicates and aluminates: American Mineralogist, v. 39, p. 92–96.

Maier, C. G., and Kelley, K. K., 1932, An equation for the representation of high temperature heat content data: American Chemical Society Journal, v. 54, p. 3243–3246.

Manning, C. E., 1994, The solubility of quartz in H_2O in the lower crust and upper mantle: Geochimica et Cosmochimica Acta, v. 58, p. 4831–4839.

Markl, G., 2001, A new type of silicate liquid immiscibility in peralkaline nepheline syenites (lujavrites) of the Ilimaussaq complex, South Greenland: Contributions to Mineralogy and Petrology, v. 241, p. 458–472.

Markl, G., Marks, M., Schwinn, G., and Sommer, H., 2001, Phase equilibrium constraints on intensive. crystallization parameters of the Ilimaussaq Complex, South Greenland: Journal of Petrology, v. 42, p. 2231–2258.

Meier, W., Olson, D., and Baerlocher, C., 2001, Atlas of zeolite structure types, Fifth Revised Edition: Amsterdam, Elsevier, 302 p.

Murdoch, J. B., Stebbins, J. F., Carmichael, I. S. E., and Pines, A., 1988, A ^{29}Si nuclear magnetic resonance study of silicon-aluminum ordering in leucite and analcite: Physics and Chemistry of Minerals, v. 15, p. 370–382.

Murphy, W. M., Pabalan, R. T., Prikryl, J. D., and Goulet, C. J., 1996, Reaction kinetics and thermodynamics of aqueous dissolution and growth of analcime and Na-clinoptilolite at 25°C: American Journal of Science, v. 296, p. 128–186.

Navrotsky, A., Rapp, R. P., Smelik, E., Burnley, P., Circone, S., Chai, L., Bose, K., and Westrich, H. R., 1994, The behavior of H_2O and CO_2 in high-temperature lead borate solution calorimetry of volatile-bearing phases: American Mineralogist, v. 79, p. 1099–1109.

Neuhoff, P. S., ms, 2000, Thermodynamic Properties and Parageneses of Rock-Forming Zeolites: Ph.D. thesis, Stanford University, Stanford, 240 p.

Neuhoff, P. S., and Stebbins, J. F., 2001, A solid solution model for Si-Al substitution in disordered FAU and LTA zeolites: Microporous and Mesoporous Materials, v. 49, p. 139–148.

Neuhoff, P. S., Watt, W. S., Bird, D. K., and Pedersen, A. K., 1997, Timing and Structural Relations of Regional Zeolite Zones in Basalts of the East Greenland Continental Margin: Geology, v. 25, p. 803–806.

Neuhoff, P. S., Fridriksson, Th., and Bird, D. K., 2000, Zeolite Parageneses in the North Atlantic Igneous Province: Implications for Geotectonics and Groundwater Quality of Basaltic Crust: International Geology Review, v. 42, p. 15–44.

Neuhoff, P. S., Stebbins, J. F., and Bird, D. K., 2003, Si-Al disorder and solid solutions in analcime, chabazite, and wairakite: American Mineralogist, v. 88, p. 410–423.

Nitkiewicz, A. M., Kerrick, D., and Hemingway, B. S., 1983, The effect of particle size on enthalpy of solution of quartz: Geological Society of America Abstracts with Programs, v. 15, n. 6, p. 653.
Ogihara, S., 1996, Diagenetic transformation of clinoptilolite to analcime in silicic tuffs of Hokkaido, Japan: Mineralium Deposita, v. 31, p. 548–553.
Ogorodova, L. P., Kiseleva, I. A., Mel'chakova, L. V., Belitskii, I. A., and Fursenko, B. A., 1996, Enthalpies of Formation and Dehydration of Natural Analcime: Geochemistry International, v. 34, p. 980–984.
Openshaw, R. E., Hemingway, B. S., Robie, R. A., Waldbaum, D. R., and Krupka, K. M., 1976, The heat capacities at low temperatures and entropies at 198.15 K of low albite, microcline and high sanidine: U.S. Geological Survey Journal of Research, v. 4, p. 195–204.
Ott, G., Karotke, E., and Althaus, E., 1986, Measurement of compressibility and high-pressure thermal expansion of minerals with a helium-pressurized heated X-ray camera: High Temperatures High Pressures, v. 16, p. 549–551.
Passaglia, E., and Sheppard, R. A., 2001, The crystal chemistry of zeolites, *in* Bish, D. L., and Ming, D. W., editors, Natural Zeolites: Occurrence, Properties, Applications: Mineralogical Society of America and the Geochemical Society Reviews in Mineralogy and Geochemistry, v. 45, p. 551–587.
Petrovic, I., and Navrotsky, A., 1997, Thermochemistry of Na-faujasites with varying Si/Al ratios: Microporous Materials, v. 9, p. 1–12.
Petrovic, I., Navrotsky, A., Davis, M. E., and Zones, S. I., 1993, Thermochemical study of the stability of frameworks in high silica zeolites: Chemistry of Materials, v. 5, p. 1805–1813.
Phillips, B. L., and Kirkpatrick, R. J., 1994, Short-range Si-Al order in leucite and analcime: Determination of the configurational entropy from ^{27}Al and variable-temperature ^{29}Si NMR spectroscopy of leucite, its Cs- and Rb-exchanged derivatives, and analcime: American Mineralogist, v. 79, p. 1025–1031.
Ransom, B., and Helgeson, H. C., 1994, Estimation of the standard molal heat capacities, entropies, and volumes of 2:1 clay minerals: Geochimica et Cosmochimica Acta, v. 58, p. 4537–4547.
Redkin, A. F. and Hemley, J. J., 2000, Experimental Cs and Sr sorption on analcime in rock-buffered systems at 250–300 °C and P_{sat} and the thermodynamic evaluation of mineral solubilities and phase relations: European Journal of Mineralogy, v. 12, p. 999–1014.
Rimstidt, J. D., 1997, Quartz solubility at low temperatures: Geochimica et Cosmochimica Acta, v. 61, p. 2553–2558.
Robie, R. A., and Hemingway, B. S., 1995, Thermodynamic properties of minerals and related substances at 298.15 K and 1 bar (10^5 pascals) pressure and at higher temperatures: United States Geological Survey Bulletin 2131, 461 p.
Saha, P., 1959, Geochemical and x-ray investigation of natural and synthetic analcites: American Mineralogist, v. 44, p. 300–313.
——— 1961, The system $NaAlSiO_4$ (nepheline)-$NaAlSi_3O_8$ (albite)-H_2O: American Mineralogist, v. 46, p. 859–884.
Seki, Y., and Oki, Y., 1969, Wairakite-analcime solid solutions from low-grade metamorphic rocks of the Tanazawa Mountains, Central Japan: Mineralogical Journal, v. 6, p. 36–45.
Shim, S. H., Navrotsky, A., Gaffney, T. R., and MacDougall, J. E., 1999, Chabazite: Energetics of hydration, enthalpy of formation, and effect of cations on stability: American Mineralogist, v. 84, p. 1870–1882.
Takaishi, T., 1998, Ordered distribution of Al atoms in the framework of analcimes: Journal of the Chemical Society-Faraday Transactions, v. 94, p. 1507–1518.
Teertstra, D. K., Sherriff, B. L., Xu, Z., and Cerny, P., 1994, MAS and DOR NMR study of Al-Si order in the analcime-pollucite series: Canadian Mineralogist, v. 32, p. 69–80.
Thompson, A. B., 1970, A note on kaolinite-pyrophyllite equilibrium: American Journal of Science, v. 268, p. 454–458.
——— 1971, Analcite-albite equilibria at low temperatures: American Journal of Science, v. 271, p. 79–92.
Thompson, J. B., Jr., Waldbaum, D. R., and Hovis, G. L., 1974, Thermodynamic properties related to ordering in end-member alkali feldspars, *in* Mackenzie, W. S., and Zussman, J., editors, The Feldspars: New York, Crane, Russak, and Company, p. 218–248.
Tingle, T. N., Neuhoff, P. S., Ostergren, J. D., Jones, R. E., and Donovan, J. J., 1996, The effect of "missing" (unanalyzed) oxygen on quantitative electron probe microanalysis of hydrous silicate and oxide minerals: Geological Society of America Abstracts with Programs, v. 28, no. 6, p. 212.
van Reeuwijk, L. P., 1974, The Thermal Dehydration of Natural Zeolites: Wageningen: H. Veenman and Zonen B.V., 88 p.
Waldbaum, D. R., and Robie, R. A., 1970, An internal sample container for hydrofluoric acid solution calorimetry: Journal of Geology, v. 78, p. 736–741.
Walker, G. P. L., 1960, Zeolite zones and dike distribution in relation to the structure of the basalts of eastern Iceland: Journal of Geology, v. 68, p. 515–528.
Walther, J. W., and Helgeson, H. C., 1977, Calculation of the thermodynamic properties of aqueous silica and the solubility of quartz and its polymorphs at high pressures and temperatures: American Journal of Science, v. 277, p. 1315–1351.
Wilkin, R. T. and Barnes, H. L., 1998, Solubility and stability of zeolites in aqueous solution: I. Analcime, Na-, and K-clinoptilolite: American Mineralogist, v. 83, p. 746–761.
Wilkinson, J. F. G., and Hensel, H. D., 1994, Nephelines and analcimes in some alkaline igneous rocks: Contributions to Mineralogy and Petrology, v. 118, p. 79–91.
Wilkinson, J. F. G., and Whetten, J. T., 1964, Some analcime-bearing pyroclastic and sedimentary rocks from New South Wales: Journal of Sedimentary Petrology, v. 34, p. 543–553.
Wise, W. S., 1984, Thermodynamic studies of zeolites: Analcime solid solutions, *in* Olson, D., and Bisio, A., editors, Proceedings of the Sixth International Zeolite Conference: Guildford, Butterworths, p. 616–623.

Wise, W. S., and Gill, R. H., 1977, Minerals of the Benitoite Gem mine: Mineralogical Record, v. 8, p. 442–52.
Wolery, T. J., and Daveler, S. A., 1992, EQ3/6. A Software Package for Geochemical Modeling of Aqueous Systems: Lawrence Livermore National Laboratory UCRL-MA-110772 PT I-IV, 66 p.
Yang, S. Y., and Navrotsky, A., 2000, Energetics of formation and hydration of ion-exchanged zeolite Y: Microporous and Mesoporous Materials, v. 37, p. 175–186.
Yoder, H. S., Jr., and Weir, C. E., 1960, High-pressure form of analcite and free energy change with pressure of analcite reactions: American Journal of Science, v. 258-A, p. 420–433.
Zhao, P., Neuhoff, P. S., and Stebbins, J. F., 2001, Comparison of FAM mixing to single-pulse mixing in ^{17}O 3Q- and 5Q-MAS NMR of oxygen sites in zeolites: Chemical Physics Letters, v. 344, p. 325–332.